Neurobiology of Disease 70 (2014) 190–203

Contents lists available at ScienceDirect

Neurobiology of Disease

journal homepage: www.elsevier.com/locate/ynbdi

Phenotypic characterization of recessive gene knockout rat models of Parkinson's disease

Kuldip D. Dave [a,*], Shehan De Silva [a], Niketa P. Sheth [a], Sylvie Ramboz [b], Melissa J. Beck [c], Changyu Quang [c], Robert C. Switzer III [d], Syed O. Ahmad [e], Susan M. Sunkin [f], Dan Walker [g], Xiaoxia Cui [h], Daniel A. Fisher [h], Aaron M. McCoy [h], Kevin Gamber [h], Xiaodong Ding [i], Matthew S. Goldberg [i], Stanley A. Benkovic [j], Meredith Haupt [a], Marco A.S. Baptista [a], Brian K. Fiske [a], Todd B. Sherer [a], Mark A. Frasier [a]

[a] The Michael J. Fox Foundation for Parkinson's Research. 498 Seventh Avenue, 18th Floor, New York, NY 10018 USA
[b] Psychogenics, Inc. 765 Old Saw Mill River Road, Tarrytown, NY 10591 USA
[c] WIL Research 1407 George Road, Ashland, OH 44805 USA
[d] NeuroScience Associates. 10915 Lake Ridge Drive, Knoxville, TN 37934 USA
[e] Saint Louis University. 3437 Caroline, Suite 3113, St. Louis, MO 63104 USA
[f] Allen Institute for Brain Science 551 N, 34th Street, Seattle, WA 98103 USA
[g] Leica Biosystems. 1360 Park Center Drive, Vista, CA 92081 USA
[h] SAGE Labs. 2033 Westport Center Drive, Saint Louis, MO, 63146 USA
[i] The University of Texas Southwestern Medical Center, 6000 Harry Hines Blvd, Dallas TX 75390 USA
[j] BNRL, 1992 River Road, Morgantown, WV 26501 USA

ARTICLE INFO

Article history:
Received 9 October 2013
Revised 30 May 2014
Accepted 13 June 2014
Available online 24 June 2014

ABSTRACT

Recessively inherited loss-of-function mutations in the PTEN-induced putative kinase 1(Pink1), DJ-1 (Park7) and Parkin (Park2) genes are linked to familial cases of early-onset Parkinson's disease (PD). As part of its strategy to provide more tools for the research community, The Michael J. Fox Foundation for Parkinson's Research (MJFF) funded the generation of novel rat models with targeted disruption ofPink1, DJ-1 or Parkin genes and determined if the loss of these proteins would result in a progressive PD-like phenotype. Pathological, neurochemical and behavioral outcome measures were collected at 4, 6 and 8 months of age in homozygous KO rats and compared to wild-type (WT) rats. Both Pink1 and DJ-1 KO rats showed progressive nigral neurodegeneration with about 50% dopaminergic cell loss observed at 8 months of age. ThePink1 KO and DJ-1 KO rats also showed a two to three fold increase in striatal dopamine and serotonin content at 8 months of age. Both Pink1 KO and DJ-1 KO rats exhibited significant motor deficits starting at 4 months of age. However, Parkin KO rats displayed normal behaviors with no neurochemical or pathological changes. These results demonstrate that inactivation of the Pink1 or DJ-1 genes in the rat produces progressive neurodegeneration and early behavioral deficits, suggesting that these recessive genes may be essential for the survival of dopaminergic neurons in the substantia nigra (SN). These MJFF-generated novel rat models will assist the research community to elucidate the mechanisms by which these recessive genes produce PD pathology and potentially aid in therapeutic development.

Introduction

Parkinson's disease (PD) is the second most common neurodegenerative disorder and is characterized clinically by tremor, rigidity, bradykinesia and postural instability. Pathologically, the disease is associated with loss of dopaminergic neurons in the substantia nigra (SN), decreased dopamine (DA) neurotransmission and the presence of neuronal intracellular Lewy body (LB) inclusions (Lees et al., 2009).While PD is a complex, multifactorial disease and largely sporadic, rare familial forms of the disease have been correlated to specific genetic mutations that are inherited in Mendelian fashion (Farrer, 2006). Mutations in alpha-synuclein (aSyn) and leucine rich-repeat kinase 2 (LRRK2) have been linked to autosomal-dominant forms of PD (Martin et al., 2011). Mutations in the Pink1, DJ-1 and Parkin genes have been causally linked to autosomal recessive PD with early age of onset, slow progression of the disease, and a more selective loss of DA neurons than that associated with sporadic late-onset PD (Houlden and Singleton, 2012). Discovery of rare familial monogenic forms of PD has provided new targets to pursue for drug

* Corresponding author.
E-mail address: kdave@michaeljfox.org (K.D. Dave).
Available online on ScienceDirect (www.sciencedirect.com).

http://dx.doi.org/10.1016/j.nbd.2014.06.009

development, and provided an impetus to generate animal models to understand the functions of these genes.

Knockout (KO) mice lacking Pink1, DJ-1 or Parkin genes show subtle behavioral and neurochemical abnormalities. For example, Pink1 KO mice exhibit decreased DA release in striatal slices and impairments in plasticity (Kitada et al., 2007)while the Parkin KO mice exhibit increased striatal extracellular DA concentration and behavioral deficits (Goldberg et al., 2003). Similarly, DJ-1 KO mice show reduced DA overflow in the striatum, dysfunction in long-term potentiation and hypoactivity (Goldberg et al., 2005). Neither nigral cell loss nor alpha-synuclein aggregation was observed in these single gene KO mice. Triple KO mice lacking Pink1, DJ-1 and Parkin genes do not exhibit abnormal behavior or reduced DA neuron number up to 24 months of age, although evoked dopamine release and striatal synaptic plasticity are impaired (Kitada et al., 2009). More recently, DJ-1 KO mice fully backcrossed to a C57BL/6 J backgrounds howed early-onset unilateral loss of nigral DA neurons, which progressed to bilateral degeneration with age (Rousseaux et al., 2012).This variability in phenotypes and lack of predictive validity to human PD has limited our understanding of the biologic function of these genes and hindered our ability to develop therapies against these targets.

The Michael J. Fox Foundation for Parkinson's Research (MJFF) directly sponsors generation, characterization, and distribution of animal models to increase availability and accessibility of these much needed tools to accelerate Parkinson's research (Baptista et al., 2013). As part of this overall strategy, MJFF funded generation of novel rat knockout models of Pink1, DJ-1, and Parkin genes using Zinc Finger Nuclease (ZFN) Technology. This technology enables rapid creation of targeted gene knockouts, genomic insertions or gene editing in eukaryotes (Geurts et al., 2009). The current study describes detailed behavioral, neurochemical and pathological characterization of these models for possible PD-like features. Results how that Pink1 KO and DJ-1 KO, but not Parkin KO rats, have early motor deficits and exhibit a progressive loss of SN DA neurons.

Methods

Generation of Pink1, DJ-1 and Parkin knockout rats

Animal husbandry

Creation and preliminary characterization of KO rats was performed at SAGE Labs, which operated under approved animal protocols overseen by SAGE's Institutional Animal Care and Use Committee (IACUC). Long Evans Hooded rats (Crl:LE) from Charles River Laboratories International Inc. (Wilmington, MA) were used for both microinjection and breeding. Long Evans rats were chosen due to better visual function observed in the pigmented strains (as opposed to albino strains) (Prusky et al., 2002), which may aid in testing for behavioral tasks that involve vision. Rats were housed in standard cages on IVC racks and maintained on a 12 h light/dark cycle with *ad libitum* access to food and water. Routine health monitoring of the colony was performed at IDEXX (Columbia, MO) and revealed no evidence of infection with serious known pathogens. Rats were housed two per cage and body weights were collected weekly. Separate groups of knockout rats or Long Evans WT rats were aged up to 4, 6, or 8 months and were sent for phenotypic characterization at one of two contract research organizations: WIL Research Labs (Ashland, OH) or Psychogenics, Inc (Tarrytown, NY).

ZFN mRNA preparation and microinjections

A pair of active ZFNs each specific for *Pink1*, *DJ-1 or Parkin* was obtained from the CompoZr product line (Sigma, St. Louis, MO). mRNA was prepared from each construct linearized with XhoI restriction enzyme and using MessageMax and Poly(A) polymerase tailing kits (Epicentre Biotechnology, Madison, WI), purified, quantified, combined (1:1 ratio), and transfected into rat C6 cells for activity validation. Four to five week-old donors were injected with 20 units of Pregnant mare serum gonadotropin (PMS) followed by 50 units of human chorionic gonadotropin (hCG) injection 48 h after the PMS injection and then immediately mated with stud males after the hCG injection. Fertilized eggs were harvested a day later for mating. ZFN mRNA was microinjected at 10 ng/μl into the pronucleus of fertilized eggs. Following microinjection, 25–30 eggs were transferred into each pseudopregnant female, which gave birth to the founder generation.

Founder identification and breeding

Tail or toe biopsies were used for genomic DNA extraction and analysis as described previously (Carbery et al., 2010). Primers flanking the target sites used for genotyping are Pink1FWD 5′-CCATGGGCAGGA ACACTATT; Pink1REV 5′-CCTACACACAGCCCTCACCT; DJ-1 FWD, 5′-TATTGGGCCTTTCTCTTGGA; DJ-1 REV, AGACAGGAGTTCATGCCA CC; Parkin FWD 5′-GGTGTCTTGGCTCAGTGTGA; and Parkin Rev 5′-GCCACCCAGAATAGCATCTC.The chosen founder was then bred to a wild type rat to obtain heterozygous rats, and sibling mating of heterozygotes resulted in homozygous knockout rats. To differentiate wild type, heterozygotes and homozygotes, 100 bp regions are amplified to distinguish the 26 bp and 8 bp deletion in size in Pink1 and DJ-1, respectively, by using Pink1 50 bp F, 5′-CCCTGGCTGACTATCC TGAC; Pink1 50 bp R, 5′-CCACCACCCACTACCACTTACT; DJ-1 50 bp F, 5′-TGGGAGTGACAGTCTCAGTGG; and DJ-1 50 bp R, 5′-AGCTATGA GGCCCTTCCTGT. Homozygous and heterozygous Parkin KO rats were confirmed to contain the 5-bp deletion by sequencing the PCR amplicon with above primers.

RNA preparation and qRT-PCR

Knockout and wild type littermates were sacrificed for tissue harvest at 5–9 weeks of age. Brain tissues were dissected and stored in RNAlater solution (Ambion, Austin, TX) at 4 °C. Total RNA was extracted using Trizol reagent (Sigma, Saint Louis, MO). First strand cDNA was synthesized from 1 μg of total RNA that had been treated using DNase (Ambion) by using the oligo$(dT)_{20}$ primer and SuperscriptIII reverse transcriptase (Life Technology, Carlsbad, CA). Reverse transcription was carried out with 1 cycle of 50 °C for 50 min and 85 °C for 5 min. qPCR analyses were carried out with 1 μL of total RNA using SYBR Green (Sigma) with forward primer (5′-CATGGCTTTGGATG GAGAGT) and reverse primer (5′-TGGGAGTTTGCTCTTCAAGG) for Pink1; forward primer (5′-CGATGTGGTTGTTCTTCCAG) and reverse primer (5′-GCCGTTCATCATTTTGTCCT) for DJ-1;and forward primer (5′-CTGGCAGTCATTCTGGACAC) and reverse primer (5′-CTCTCCAC TCATCCGGTTTG) for Parkin. β-Actin was used as the reference gene amplified with forward primer (5′-GGCATCCTGACCCTGAAGTA) and reverse primer (5′-GGGGTGTTGAAGGTCTCAAA). qPCR were carried out using 1 cycle of 94 °C for 2 min followed by 40 cycles of 94 °C for 15 sec and 60 °C for 30 sec for amplification. The data were presented as relative gene expression and were calculated using BioRad software ($\Delta\Delta C_t$).

Western blot

Male KO and WT littermates were sacrificed for tissue harvest at 5–9 weeks of age. Brain and heart tissues were dissected and immediately frozen in liquid nitrogen and stored at −80 °C. Tissues were dounce homogenized in 400 μL RIPA buffer (Sigma) ± 4× Protease inhibitor cocktail (Sigma) and incubated on ice for 1 hour with 15 second vortexing every 15 minutes. Then, the homogenate was centrifuged at 14000 X g for 5 min at 4 °C. Supernatant was then mixed with an equal volume of 2× Laemmli buffer (Sigma). Samples were denatured at 100 °C for 5 minutes before loading. After denaturation, 15 μL of lysate was loaded on a TGX 4–20% precast gel (Bio-Rad) and electrophoresed at 200 V for 25 minutes. The resolved gel was transferred to 0.45 μm nitrocellulose membrane (Bio-Rad) by wet transfer apparatus (Bio-Rad) for 60 min at 100 V. The transfer buffer contained standard tris-glycine salts, 20% MeOH, and 0.25% SDS. Transfer efficiency was analyzed using a Ponceau S (Sigma) stain. The membrane was then

washed 2× for 5 min with water and blocked for 60 min in Western Block solution (Sigma). After blocking, the membrane was washed 3× for 5 min in 1× TBS-T and incubated for 60 min in primary antibody solution (DJ-1 antibody, Sigma, #SAB4500248, at 1:1000 dilution in Western Block solution). After the incubation, the membrane was washed 5× 5 min in 1× TBS-T and incubated with the secondary antibody (Jackson Immunolab, goat-anti rabbit, at 1:50,000 dilution) for 30 min. The membrane was washed 5× in 1× TBST-T and incubated for 2 min in Supersignal West Pico substrate (Thermo Scientific, Waltham, MA) and visualized on a ChemiDoc XRS ± (Bio-Rad). β-Actin was used as internal control for normalizing total input proteins. Parkin western analysis was performed on brain homogenates from wild-type and Parkin KO rats essentially as described above, using rabbit anti-Parkin (#2132, Chemicon) and mouse anti-Parkin (MAB5512, Millipore).

Detailed characterization of KO rats – behavior, neurochemistry and pathology

Behavioral phenotyping at WIL research labs

Upon arrival from SAGE Labs, all animals were gang-housed in the same way (2 per cage), in clean, wire-mesh cages suspended above cage-board. Rats were housed throughout the acclimation period (at least 5 days) and during the behavioral testing phase in an environmentally controlled room. Controls were set to maintain a temperature of 20–23 °C, a relative humidity of approximately 30–70%, and a 12-h light/12-h dark photoperiod. The basal diet used in these studies, PMI Nutrition International, LLC, Certified Rodent LabDiet 5002, is a certified feed with appropriate analyses performed by the manufacturer and provided to WIL Research. Reverse osmosis-treated (on-site) drinking water, delivered by an automatic watering system, was provided ad libitum throughout the study period. The protocols were reviewed and approved by the WIL Research Institutional Animal Care and Use Committee (IACUC).Animals were maintained in accordance with the "Guide for the Care and Use of Laboratory Animals" (National Research Council, 1996).On the first behavioral testing day, male homozygous knockouts of Pink1, DJ-1, Parkin or LE WT (n = 15/group/age) were first tested for behavioral deficits in the functional observational battery (FOB) test followed at least an hour later in the accelerating rotarod test paradigm. Rats were subjected to rotarod for 4 additional days (for a total of 5 days). The 15 rats/group were then randomized into 2 subsets. Subset A consisted of 9 rats which were assigned for neuropathology. Subset B consisted of 6 rats which were assigned to neurochemistry.

Behavioral phenotyping at Psychogenics, Inc.

During the course of the study, 12 /12 light/dark cycles and a room temperature of 20 to 23 °C were maintained with relative humidity maintained around 50%. Food and water were provided *ad libitum* for the duration of the study. Wet feed was also provided to animals when their body weight declined or when they displayed hindlimb deficits. Animals were monitored for survival and health statuses twice per day and body weighed once per week for the duration of the study. For these experiments, male homozygous knockouts of Pink1, DJ-1 and LE WT rats (n = 7/group) were tested at 4 months of age for their motor performance in the Tapered balance beam test, grip-strength, open-field apparatus, and NeuroCube. The same animals were then re-tested at 6 and 8 months of age.

Behavioral outcome measures

Functional observational battery (FOB). Testing was performed by the same technicians, whenever possible, without knowledge of the animals' group assignment. The FOB was performed in a sound-attenuated room equipped with a white noise generator set to operate at 70 ± 10 dB. All animals were observed for the following parameters: home cage observations [posture, convulsions/tremors, feces consistency, biting, palpebral (eyelid) closure]; handling observations (ease of removal from cage, lacrimation/chromodacryorrhea, piloerection, palpebral closure, eye prominence, red/crusty deposits, ease of handling animal in hand, salivation, fur appearance, respiratory rate/character, mucous membranes/eye/skin color, muscle tone), open field observations (evaluated over a 2-min observation period) (mobility, rearing, convulsions/tremors, grooming, bizarre/stereotypic behavior, time to first step, gait, arousal, urination/defecation, gait score, backing),sensory observations (approach response, startle response, pupil response, forelimb extension, air righting reflex, touch response, tail pinch response, eyeblink response, hindlimb extension, olfactory orientation), neuromuscular observations (hindlimb extensor strength, hindlimb foot splay, grip strength-hind and forelimb, rotarod performance), and physiological observations (catalepsy, body temperature, body weight).

NeuroCube® (NC). The NeuroCube® system is a platform that employs computer vision to detect changes in gait geometry and gait dynamics in rodents. The NC apparatus used in the current study was a circular arena (76.2 cm wide and 7.6 cm high), where the rats were allowed to walk in a circle. Rats were first allowed to acclimate in the experimental room for 1 h prior to test. Following acclimation to the test room, rats were placed in the NC system and allowed to walk in the apparatus for a 5-min session. Digital videos of the rats were processed using proprietary computer vision algorithms to extract behavioral characteristics (features) that were further fed into a machine learning algorithm that quantified phenotype differences (as described in Appendix A). Splay, stride/swing duration, base length/width, paw position coordinates, paw pressure distribution and body contour movement are examples of the 124 total features that NeuroCube platform is capable to capture. These features together constitute a quantifiable "phenotypic signature" for each group of rats which can be also visualized for quick qualitative assessment (e.g. a heat map of paw placement – see Fig. 5).

Tapered balance beam (TBB). TBB consists of a strip of smooth black acrylic 165 cm in length, with a square cross section that tapers from a width of 6 cm to 1.5 cm. The surface of the beam was covered with a thin layer of rubber to provide traction. A safety ledge (0.5 cm) was located 2 cm below the beam. The ledge maintained a constant width of 0.5 cm as the beam tapers. The angle of the beam was 17° from horizontal, running from low to high. The highest point of the beam was ~58 cm from the floor. At the "end" portion of the balance beam, there was a goal box, which rests on the aforementioned support stand. The goal box was constructed from black acrylic, measuring 25 cm^3 and containing a 10 cm^2 entrance hole. Padding under the beam was used in the event that the rat fell from the beam during testing. The padding consisted of IACUC- and veterinarian-approved disposable padded material that can be sanitized and covered by an absorbent pad. Rats received 1 training day, prior to their first Tapered Beam Test. The training day consisted of 4 training runs in the morning (AM) and 2 additional training runs in the afternoon (PM). On the day of testing, rats were allowed to acclimate to the experimental room for at least 1 hour. The TBB Test consisted of 3 consecutive runs. Rats were placed in the goal box for 5 min. The rat was then placed at the bottom of the beam and allowed to migrate to the goal box. A 30 second rest period in the goal box was provided between runs. The time to traverse the beam and the number of foot slips were recorded.

Grip strength (GS). Rats, held by their tails, were gently pulled across two push-pull gauges (San Diego Instruments, San Diego, CA) – one for their forelimb and one for their hindlimb. The grip force for the forelimbs and hindlimbs were recorded on their respective gauges. Animals were tested in three consecutive grip strength trials, with approximately 1 minute between each trial.

Open field (OF). The automated open field test was used to measure the locomotor activity (distance traveled) and rearing frequency of the rats. Animals were tested for 1 hour sessions. The open field

chambers consisted of standard rat cages that fit inside 2 steel frames (9.5 × 18 inches) that were designed with a two dimensional 4 x 8 inch beam grid to monitor horizontal and vertical locomotor activity. The activity was recorded by an automated system that counts successive photobeam breaks. The rearing frequency and distance traveled were recorded.

Accelerating Rotarod. Prior to study day 0, all rats were trained on a Rotarod device (Omni-rotor treadmill, AccuScan Instruments, Inc., Columbus, OH) for 2 minutes to acclimate to the equipment. During training, the rotation rate was set at 12 rpm. Each rat was placed on the 7 cm diameter treadmill facing opposite the direction of the rotation, and the time to the first fall and numbers of falls were recorded. Accelerating Rotarod performance was monitored once daily (1 trial/day) for 5 consecutive days, beginning on the first day of behavioral testing. Testing was performed in a sound-attenuated room equipped with a white-noise generation system set to 70 ± 10 db. For each daily trial, the rat was first placed on the treadmill as described above, and then the Rotarod, set to increase at a constant acceleration rate from 0 to 40 rpm over a period of 60 seconds, was activated. When the animal fell from the treadmill, the device was stopped, and the time on the treadmill (latency to drop) was recorded.

Neurochemical characterization of Pink1, DJ-1 and Parkin KO rats

Striatum tissues were surgically removed from euthanized animals. After weighing, tissue samples were immediately flash frozen with liquid nitrogen and stored frozen at approximately 70 °C until sample processing. During analysis, tissue samples were homogenized on wet ice with ice-cold 0.1% formic acid using a Kontes micro grinder at a ratio of 1:9 [mg (weight): μL]. For the analysis of rat striatum samples, aliquots of 50.0 μL of homogenates were added to a 96-well sample plate (2-mL well size), followed by 50 μL of 0.1% formic acid solution containing internal standards. The samples were further diluted with 350 μL of ice cold 0.1% formic acid (total 450 μL). Aliquots (200 μL) of the diluted samples were transferred and filtered through a SupelcoHybridSPE® plate for the positive ion analysis (NE, DA, 5-HT, and 5-HIAA). Second portions (200 μL) of the diluted samples were filtered through a Whatman filter plate for the negative ion analysis (DOPAC and HVA). Because of limited sample size for mouse striatum tissues (6–28 mg), Whatman filter plates were used to prepare the diluted homogenates for both positive ion and negative ion modes of analysis. Stock solutions of neurotransmitters were prepared in ice-cold 0.1% formic acid at a concentration of 1.00 mg/mL, and the stocks were sub-aliquoted into tubes (0.50 mL each) and stored at −80 °C. Calibration standards were prepared from the stock solutions with ice-cold 0.1% formic acid at various concentrations on the day of the analysis. Quality control samples were prepared in charcoal treated (2×) rat brain homogenates spiked with neurotransmitters at four concentration levels (LLQC, LQC, MQC, HQC). Quality control samples were sub-aliquoted into tubes and stored at −70 °C. Triple-stage Quadrupole mass spectrometer (API-4000) coupled with Waters Acquity UPLC® systems were used for UPLC-MS/MS analysis.

Pathological characterization of Pink1, DJ-1 and Parkin KO rats

Perfusion

Animals were deeply anesthetized by an intraperitoneal injection of sodium pentobarbital (75 mg/kg) and perfused in situ. The rats were flushed with approximately 75 mL of sodium cacodylate wash solution then perfused with approximately 225 mL of sodium cacodylate-based 4% paraformaldehyde. The brains remained in the skull for approximately 24 hours at approximately 4 °C in sodium cacodylate-based 4% paraformaldehyde. Approximately 24 hours after perfusion, the brains (including olfactory bulbs) were removed, weighed, and the size were recorded. The intact brains were placed into sodium cacodylate-based 4% paraformaldehyde for approximately 24 hours at approximately 4 °C, and then placed into phosphate-buffered saline for a minimum of 24 hours and maintained at approximately 4 °C until transport. Brains were shipped under ambient conditions to NeuroScience Associates.

Embedding and sectioning

Animal brains were received at NeuroScience Associates, treated overnight with 20% glycerol and 2% dimethylsulfoxide to prevent freeze-artifacts, and multiply embedded in a gelatin matrices using MultiBrain® Technology. After curing, the blocks were rapidly frozen by immersion in isopentane chilled to −70 °C with crushed dry ice, and mounted on the freezing stage of an AO 860 sliding microtome. The MultiBrain® blocks were sectioned in the coronal plane at 40 μ. All sections were collected sequentially into 24 containers per block that were filled with Antigen Preserve solution (49% PBS pH 7.0, 50% Ethylene glycol, 1% Polyvinyl Pyrrolidone). Sections not stained immediately were stored at −20 °C.

Immunohistochemistry

For immunochemistry, the sections were stained free-floating. For tyrosine hydroxylase staining, rabbit Anti-TH primary antibody (Pelfreeze, Cat #P40101-0)) was used at 1:6000 dilution, and secondary antibody was the goat anti-rabbit IgG-biotin at 1:238 dilution (Vector Laboratories, Catalog # BA-1000). For alpha-synuclein staining, mouse anti-aSyn primary antibody (BD Pharmingen, Catalog # 610786) was used at 1:5000 dilution, and secondary antibody was the horse anti-mouse IgG-biotin at 1:238 dilution (Vector Laboratories, Cat# BA-2001). All incubation solutions from the blocking serum onward used Tris buffered saline (TBS) with Triton X-100 (TX) as the vehicle; all rinses were with TBS. Endogenous peroxidase activity was blocked by 0.9% hydrogen peroxide treatment and non-specific binding was blocked with 1.26% whole normal serum. Following rinses, the sections were immunostained with a primary antibody overnight at room temperature. Vehicle solution contained 0.3% Triton X-100 for permeabilization. Following rinses, sections were incubated in a biotinylated secondary antibody for two hours at room temperature. Sections were incubated with an avidin-biotin-HRP complex (Vectastain Elite ABC kit, Vector Laboratories, Burlingame, CA) for one hour at room temperature. Following rinses, the sections were treated with diaminobenzidine tetrahydrochloride (DAB) and 0.0015% hydrogen peroxide to create a visible reaction product, mounted on gelatinized (subbed) glass slides, air-dried, dehydrated in alcohols, cleared in xylene, and coverslipped with Permount.

Stereology

Stereology method and validation have been recently described in detail (Healy-Stoffel et al., 2013). The *Stereologer* software package (Stereology Resource Center, Baltimore INC, Baltimore, MD) was used to estimate neuronal number with a Nikon Eclipse 80i microscope, connected with a Sony 3CCD Color Digital Video Camera, which operated an Advanced Scientific Instrumentation MS-2000 motorized Stage input into a Dell Precision 650 Server and a high resolution plasma monitor. Using design-based stereology, the number of TH-positive neurons was quantified in the SNpc of the rats. For the estimation of neuronal number, every 8thsection containing the SNpc (Bregma −2.54 to −3.88 mm) was selected from a random initial sort, described as systemic-random sampling. The section sampling fraction (ssf) was 1/8 (West et al., 1991).In design-based stereology, the optical disector method provides an equal probability for each neuron to be counted in the estimation of the total number of neurons. The counting process was as follows: First, each section was checked at low magnification (4×) and the area of interest was precisely outlined using a stereotaxic atlas of the rat brain. After outlining, the software applied systematic random grids to select counting frames on the area of interest. In each counting frame, TH-positive neurons were counted

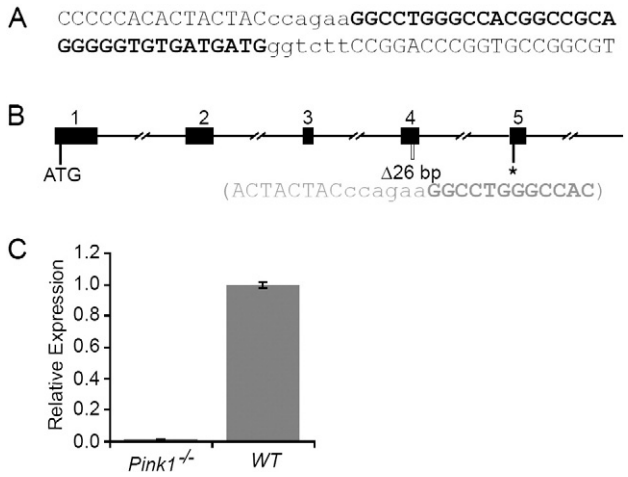

Fig. 1. Targeting in exon 4 of the *Pink1* gene. A. ZFN recognition site sequence. The two ZFN binding sites are in bold uppercase. Cleavage site is in lower case. B. Schematic of the gene structure of the first 5 exons of the *Pink1* gene. Exons are shown in filled rectangles with exon number above. ATG, position of the translational start codon; Δ26 bp marks the position of the 26 bp deletion in the colony, with nucleotide sequence below. * indicates premature stop codons introduced by the 26 bp deletion in exon 5. C. qRT-PCR analysis showing relative expression levels in wild type (*WT*) and Pink knockout ($Pink1^{-/-}$) rats.

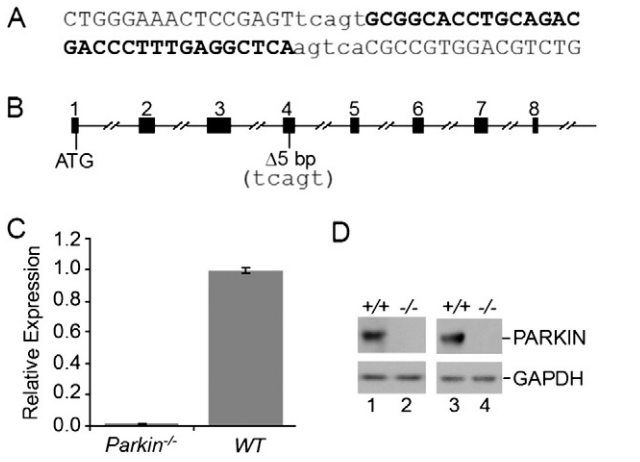

Fig. 3. Targeting in exon 4 of the *Parkin* gene. A. ZFN recognition site sequence. The two ZFN binding sites are in bold uppercase. Cleavage site is in lower case. B. Schematic of the gene structure of the *Parkin* gene. Exons are shown in filled rectangles with exon number above. ATG, position of the translational start codon; Δ5 bp marks the position of the 5 bp deletion in the colony, with nucleotide sequence below. C. qRT-PCR analysis showing relative expression levels in wild type (*WT*) and *Parkin* knockout ($Parkin^{-/-}$) rats. D. Western blots on PARKIN protein levels in wild type (+/+) and *Parkin* knockout (−/−) rats, with GAPDH as loading control. Lanes 1 and 2 are rat brain cortex homogenate blotted using anti-PARKIN antibody #2132, and lanes 3 and 4, with anti-PARKIN antibody #MAB5512.

at high magnification with a 100×/1.4 aperture oil immersion lens (yielding 3600×) by the optical disector principle, which utilizes the disector probe (Sterio, 1984) in combination with optical sectioning of the z-axis (or optical fractionator method) (West et al., 1991). In the counting rule of the optical disector, a neuron was counted only if nucleoli came into focus within the counting frame without touching the exclusion lines. The top and bottom of the sample tissue were covered with a guard volume, which avoids an artificial effect created from cutting the section with blade. This is called "capping" or cutting the neurons in half. The guard height of the present study was at least 3 μm in top and bottom (however, it could be as high as 4 μm depending on the tissue thickness), as measured by linear encoder. The 10–12 μm middle of 18–21 μm thick sample was analyzed. The thickness of each section was determined by the mean thickness of count frames measured by a 100×/1.4 aperture oil immersion lens and a linear encoder. After every sample section was analyzed, the total number of TH-positive neurons in the interest area (N) was estimated by multiplying the number of counted neurons (ΣQ) by the reciprocals of three sample fraction such as the section sampling fraction (ssf), the area sampling fraction (asf), and the section thickness sampling fraction (stsf). The *Stereologer* software package (Stereology Resource Center, Baltimore INC, Baltimore, MD) calculated the total neuronal number.

$$N = \sum Q \times \left(\frac{1}{ssf}\right) \times \left(\frac{1}{asf}\right) \times \left(\frac{1}{stsf}\right)$$

The average number of slides varied from 5–7 per animal and the Coefficient of Error (CE) was capped at .15 with the actual mean value of 0.07.

Statistical analyses. Data throughout the paper are expressed as mean average ± SEM for a given sample size. Statistical analysis was performed by means of, when appropriate, either a one-way analysis of variance (ANOVA) or a two-way analysis of variance with age and genotype as the two variables. Post-hoc tests (Dunnett's test for one-way ANOVA and Bonferroni multiple comparisons test for two-way ANOVA)were used with significance set at $p < 0.05$.

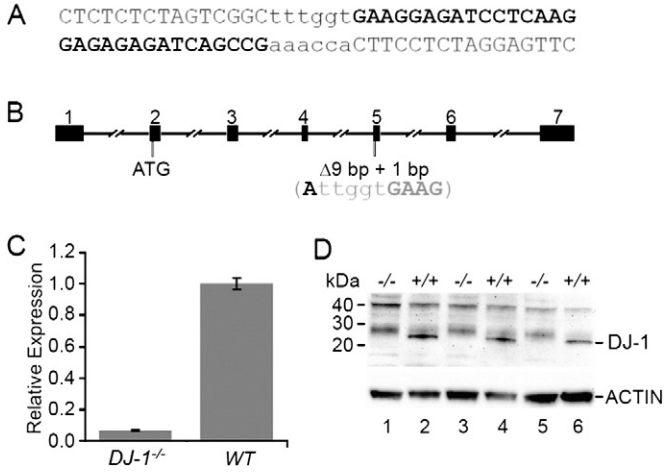

Fig. 2. Targeting in exon 5 of the *DJ-1* gene. A. ZFN recognition site sequence. The two ZFN binding sites are in bold uppercase. Cleavage site is in lower case. B. Schematic of the gene structure of the *DJ-1* gene. Exons are shown in filled rectangles with exon number above. ATG, position of the translational start codon; Δ9 bp ± 1 bp marks the position of the 9 bp deletion with 1 bp insertion in the colony, with nucleotide sequence below. * indicates premature stop codons introduced by the in/del in exon 6. C. qRT-PCR analysis showing relative expression levels in wild type (*WT*) and *DJ-1* knockout ($DJ\text{-}1^{-/-}$) rats. D. Western blots on DJ-1 protein levels in wild type (±/±) and *DJ-1* knockout (−/−) rats, with actin as loading control. Lanes 1, 3 and 5 are striatum lysis from three individual knockout rats, and lanes 2, 4 and 6 are striatum lysis from three individual wild type rats. Molecular weight standard is shown on the left and protein identity, on the right.

Results

Generation of KO rats

MJFF partnered with SAGE Labs (St. Louis, MO) to generate novel rat models with ZFN-mediated targeted disruption of genes with mutations causally linked to PD through human genetic studies. ZFNs are fusion proteins of a zinc finger protein and DNA endonuclease domain of a type II restriction enzyme, *Fok*I (Geurts et al., 2009). ZFNs are engineered to specifically bind and cleave at specific chromosomal loci to generate double strand breaks, repair of which by the non-

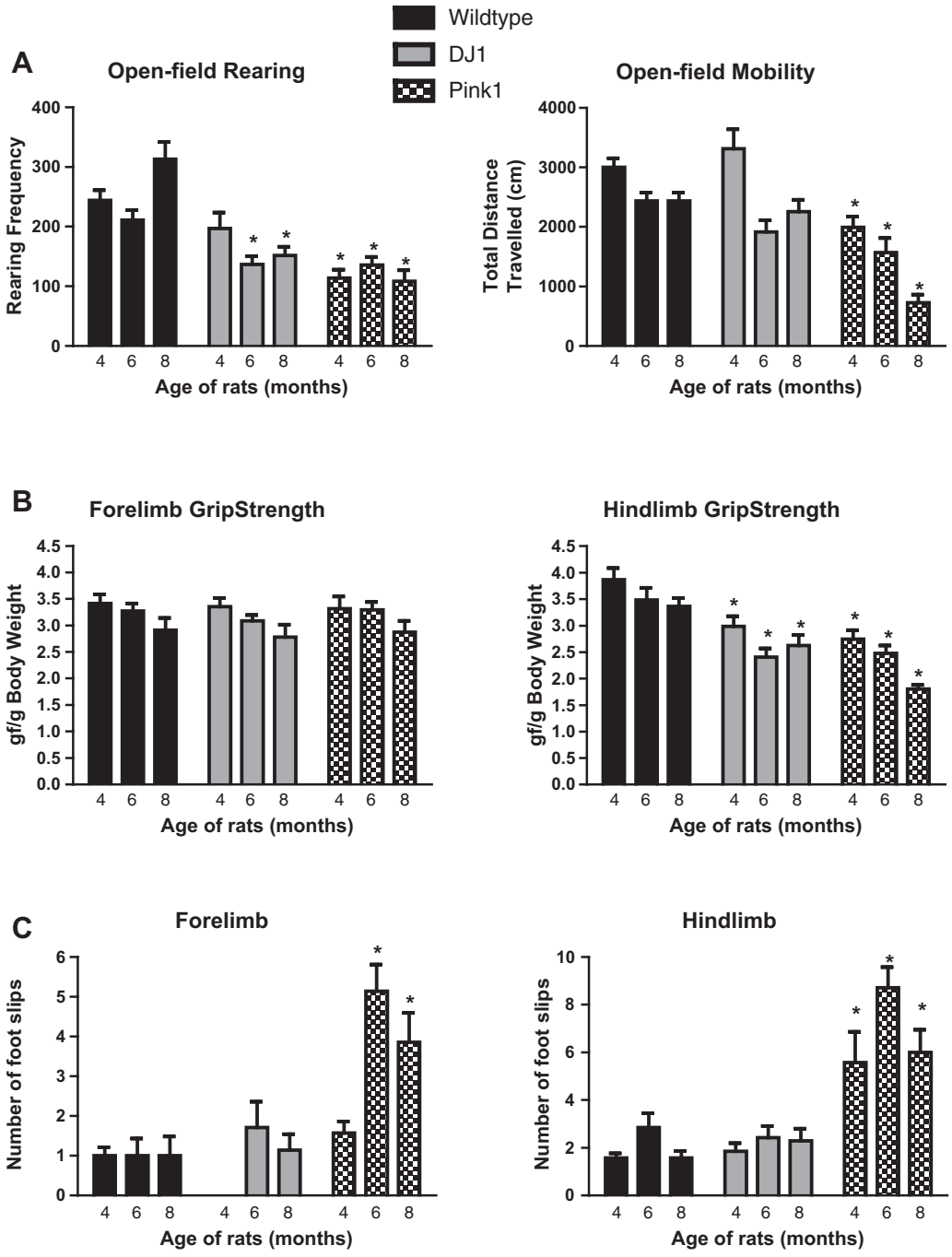

Fig. 4. Pink1 and DJ-1 KO rats display behavioral abnormalities. Homozygous Pink1 KO (n = 7), homozygous DJ-1 KO (n = 7) and Long Evans wild type rats (n = 7) were tested at 4, 6 and 8 months of age. (A) Motor Movements: Automated open field apparatus consisting of photobeam breaks to monitor horizontal and vertical locomotor activity was used to measure rearing frequency (Left) and total distance travelled (Right). (B) Motor Strength: Grip Strength was measured by obtaining grip force on push-pull gauges for both the forelimb (Left) and hindlimb (Right). An average was taken for three consecutive grip strength trials, with 1 minute between each trial. (C) Motor Coordination: Numbers of foot slips were measured in a tapered balance beam apparatus. Rats were placed at the bottom of the beam and allowed to migrate up to the goal box which was 58 cm from the floor. The numbers of forelimb (Left) and hindlimb (Right) foot slips were recorded. An average was taken for three consecutive runs, with 30 seconds between each trial. *P < 0.01, significantly different from wild type, 2-way Repeated Measures ANOVA, followed by Bonferroni multiple comparisons. Data are represented as means ± SEM.

homologous end joining pathway results in insertions/deletions that potentially disrupt the gene function (Gaj et al., 2012). A pair of ZFNs were each designed and confirmed to cleave within exon 4 of the *Pink1* gene, exon 5 of the *DJ-1* gene and exon 4 of the Parkin gene (Figs. 1A, 2A and 3A). A founder with a 26-bp deletion in the Pink1 exon 4, a founder carrying a 9-bp deletion along with a 1-bp insertion in the DJ-1 gene, and a founder containing a 5-bp deletion in the Parkin gene were bred to establish a colony for each of the knockout models. All three mutations led to a frame-shift that resulted in a premature stop codon in the exon immediately following (Figs. 1B & 2B). Quantitative RT-PCR detected very little mRNA in homozygous animals of either Pink1 or DJ-1rats (Figs. 1C & 2C) indicating that the deletion mutations also destabilized the mRNA. Parkin mRNA levels were decreased approximately 50% in *Parkin* KO rats (Fig. 3C) indicating that this transcript

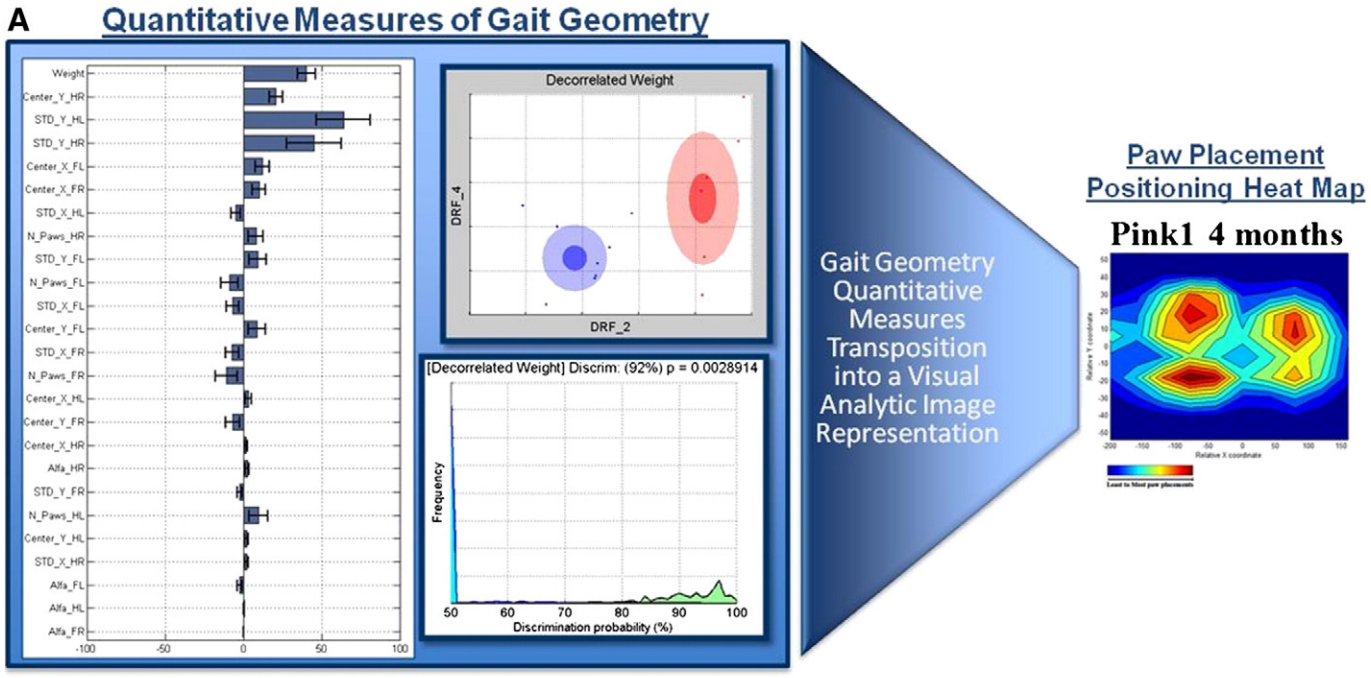
A
Quantitative Measures of Gait Geometry
Weight
Center_Y_HR
STD_Y_HL
STD_Y_HR
Center_X_FL
Center_X_FR
STD_X_HL
N_Paws_HR
STD_Y_FL
N_Paws_FL
STD_X_FL
Center_Y_FL
STD_X_FR
N_Paws_FR
Center_X_HL
Center_Y_FR
Center_X_HR
Alfa_HR
STD_Y_FR
N_Paws_HL
Center_Y_HL
STD_X_HR
Alfa_FL
Alfa_HL
Alfa_FR
-100 -50 0 50 100
Decorrelated Weight
DRF_4
DRF_2
[Decorrelated Weight] Discrim: (92%) p = 0.0028914
Frequency
50 60 70 80 90 100
Discrimination probability (%)
Gait Geometry Quantitative Measures Transposition into a Visual Analytic Image Representation
Paw Placement Positioning Heat Map
Pink1 4 months

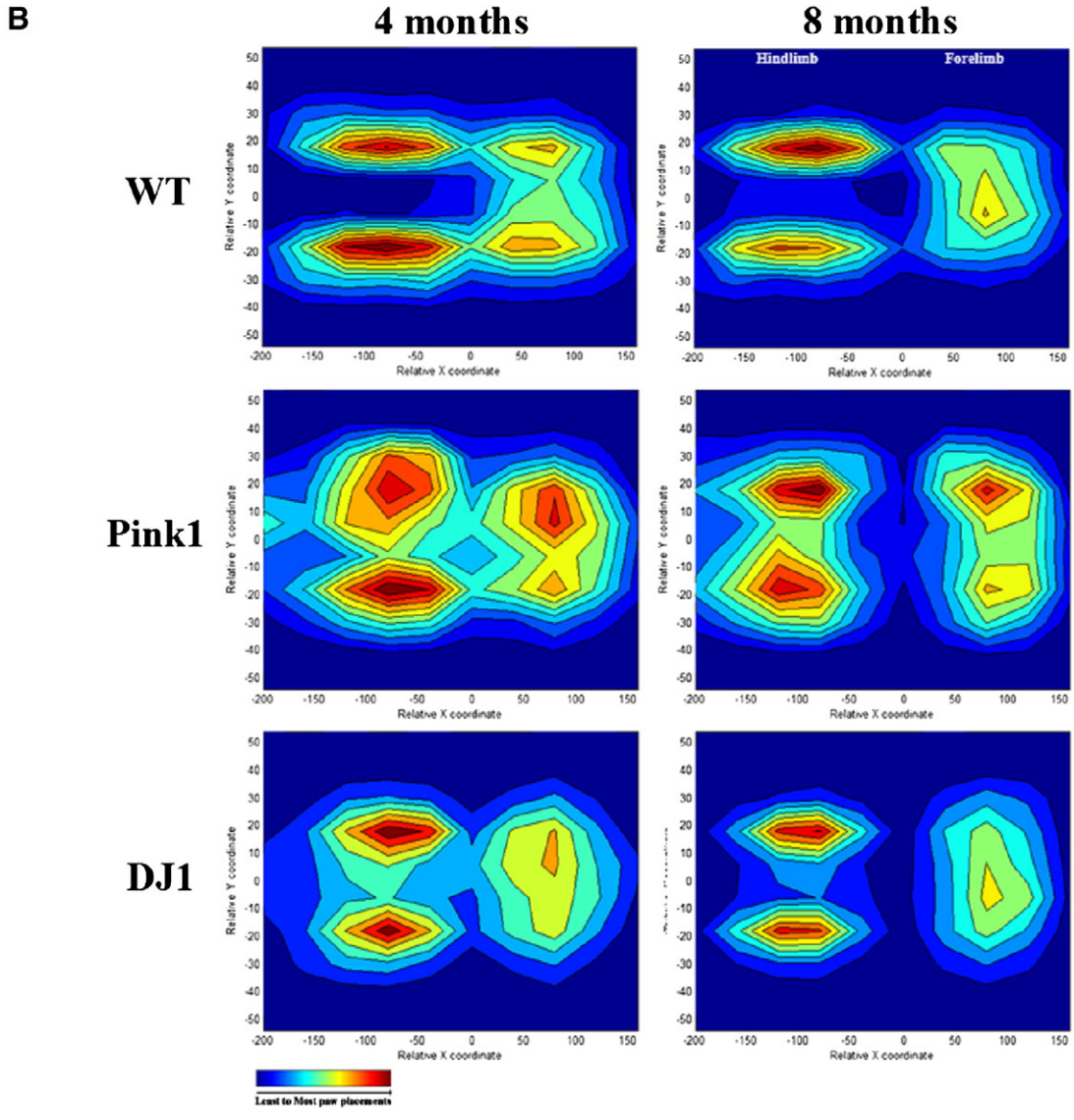
B
4 months
8 months
Hindlimb
Forelimb
WT
Pink1
DJ1
Relative Y coordinate
Relative X coordinate
-200 -150 -100 -50 0 50 100 150
50 40 30 20 10 0 -10 -20 -30 -40 -50
Least to Most paw placements

was also destabilized, but not completely, consistent with Parkin KO mice (Goldberg et al., 2003). Western blots confirmed that *DJ-1* knockout rats in fact lack DJ-1 protein (Fig. 2D). Western blots with two different epitope-mapping antibodies showed that Parkin KO rats did not contain any detectable Parkin protein (Fig. 3D). We were unable to confirm lack of Pink1 protein due to lack of specific antibodies against Pink1 protein. These homozygous gene knockouts were not embryonically lethal, and appeared to be normal at birth. In agreement with the qRT-PCR data, PCR array analysis on the expression levels of genes involved in PD pathways in all three knockout rat models confirmed specific and significant reduction of the target mRNA in DJ-1 and Pink1 knockout rats, whereas Parkin mRNA was only halved (Sun et al., 2013). No other genes were substantially altered at the mRNA level.

Behavioral phenotyping of KO rats

To investigate if loss of Pink1, DJ-1 or Parkin in the rats results in behavioral alterations, we performed systematic and detailed characterization at 4, 6 and 8 months of age. Separate groups of rats ($n = 15$/age/genotype) were tested in the functional observational battery (FOB) assay, accelerating rotarod and gait measures at Wil Research. There were no significant differences observed in the following outcome measures for any of the genotypes at any of the three ages (data not shown): convulsions/tremors, feces consistency, biting, palpebral (eyelid) closure, ease of removal from cage, lacrimation/chromodacryorrhea, piloerection, eye prominence, red/crusty deposits, ease of handling animal in hand, salivation, fur appearance, respiratory rate/character, mucous membranes/eyes/skin color, grooming, bizarre/stereotypic behavior, time to first step, urination/defecation, backing, approach response, startle response, pupil response, touch response, tail pinch response, eyeblink response, body temperature or catalepsy. Additionally, there were no significant differences observed in latency to drop in the accelerating rotarod paradigm at any of the ages tested (data not shown).

Both Pink1 and DJ-1 KO rats, but not Parkin KO rats, showed impaired gait and motor features in subjective outcome measures. Six out of fifteen Pink1 KO rats exhibited impaired gait movement, and air-righting reflex at 8 months of age(data not shown). Similarly, five out of fifteenDJ-1 KO rats showed impairment in gait and air-righting reflex at 8 months of age. Pink1 and DJ-1 KO rats exhibited normal gait and air-righting reflex at 4 and 6 months of age. Additionally, at 8 months of age, 13 out of 15 Pink1 KO rats and 9 out of 15 DJ-1 KO rats showed lack of hind-limb extensor strength and lack of overall muscle tone (data not shown). The affected rats appeared to drag hindlimbs while ambulating which could be observed in both the open-field and in the home-cage environment. Parkin KO rats were not impaired in any of the outcome measures tested. There was no increase in mortality rate despite the gait and motoric deficits observed in Pink1 and DJ-1 KO rats up to 8 months of age.

To follow up on the dysfunction in the behavioral measures observed in Pink1 and DJ-1 KO rats in WIL Research studies, a different group of homozygous Pink1 and DJ-1 KO rats ($n = 7$/genotype) were further tested at Psychogenics Inc. in more extensive behavioral assays including mobility in the open-field, rearing frequency, grip strength, tapered balance beam performance, and NC gait apparatus. In this study, the same Pink1 and DJ-1 KO rats were re-tested at 4, 6 and 8 months of age. Parkin KO rats were not tested in these additional behavioral studies due to the lack of any gait/motor phenotype in the preliminary studies at WIL Research. There was a robust reduction in the rearing frequency in both Pink1 KO and DJ-1 KO rats compared to WT rats with significant main effect for genotype, $F(2, 18) = 27.59$, $p < 0.0001$, but not with age $F(2, 36) = 2.72$, $p = 0.07$ (Fig. 4A). There was significant interaction between age and genotype for rearing frequency $F(4, 36) = 5.76$, $p = 0.0011$ with more than 50% reduction observed at 8 months of age in both genotypes. There was also a significant reduction in total distance travelled in the Pink1 KO rats at all ages with 70% decrease in mobility observed at 8 months of age, but not in the DJ-1 KO rats (Fig. 4A). There was a significant main effect for both age $F(2, 36) = 23.68$, $p < 0.0001$, and genotype $F(2, 18) = 25.53$, $p < 0.0001$, and significant interaction $F(4, 36) = 3.90$, $p = 0.0099$. Motor strength in KO vs. WT rats, as measured by limb grip strength showed no significant main effects in age, genotype or interaction in forelimb grip strength (Fig. 4A). However, hindlimb grip strength was greatly impaired with significant main effect for age $F(2, 36) = 17.10$, $p < 0.0001$, for genotype $F(2, 18) = 19.91$, $p < 0.0001$ and significant interaction $F(4, 36) = 3.24$, $p = 0.0226$ (Fig. 4B). Interestingly, deficit in hindlimb grip strength was present as early as 4 months of age and persisted through 8 months of age. Motor coordination was measured by counting the number of forelimb and hindlimb foot slips in the tapered balance beam paradigm. There was significant dysfunction of motor coordination in Pink1 KO rats, but not the DJ-1 KO rats, as compared to WT (Fig. 4C). The number of forelimb foot slips increased five-fold in both 6 and 8 month old Pink1 KO rats with significant main effects for age $F(2, 36) = 9.03$, $p < 0.0001$, for genotype $F(2, 18) = 35.79$, $p < 0.0001$, and significant interaction $F(4, 36) = 3.09$, $p = 0.0278$. The 4 month old Pink1 KO rats were not significantly different from WT. In contrast, the number of hindlimb foot slips in the balanced beam increased 3–5 fold at all three ages in Pink1 KO rats (Fig. 4C). There was a significant main effect for age $F(2, 36) = 5.19$, $p = 0.0105$, for genotype $F(2, 18) = 39.41$, $p < 0.0001$, but no significant interaction of age and genotype $F(4, 36) = 1.26$, $p = 0.3020$. Similar to forelimb foot slips, there were no significant differences in the DJ-1 KO rats compared to WT in the hindlimb foot slips.

Wild type rats weighed 469 g ± 11.9, 548 g ± 14.5, and 587 g ± 18.4 for 4, 6, and 8 months respectively. DJ-1 KO rats weighed 471 g ± 14.8, 532 g ± 18.0, and 556 g ± 23.7 for 4, 6, and 8 months respectively. Pink1 KO rats were heavier than WT counterparts with 551 g ± 15.0, 653 g ± 20.5, and 651 g ± 27.8 for 4, 6, and 8 months respectively. There were significant main effect for age $F(2, 36) = 121.03$, $p < 0.0001$, and for genotype $F(2, 18) = 9.12$, $p = 0.0018$, but no significant interaction $F(4, 36) = 2.56$, $p = 0.0547$. Gait was measured using NC apparatus looking at geometry and dynamic features. Both DJ-1 KO rats and Pink1 KO rats even at 4 months of age show substantial gait dysfunction compared to WT (Fig. 5). By looking at paw placement (part of gait geometry),

Fig. 5. Pink1 and DJ-1 KO rats display dysfunction in paw positioning and gait- Fig. 5A explains the paw positioning heat map generation: Gait geometry features are captured from each animal of each genotype at each age time point which are compiled and graphed as a bar graph representing phenotype difference for each of the feature values represented of genetically modified animal (here Pink1 KO at 4 month of age) from WT control age matched animals. Features are ranked in their ability to discriminate Pink1 KO and WT groups using PsychoGenics proprietary algorithm and feature value differences on the bar graph are shown in their ranked order from top to bottom (left pane). De-correlated statistically combinations of these original features were formed and the scatter plots of animals from each group in the axes of the two most discriminative (new) combined features (right upper plane). The overlap of the Gaussians approximating each group in this new feature space served as a measure of similarity as described in Appendix A. Contribution from each new feature to the overlap calculation was weighted by the corresponding weight of that feature and the statistical significance of the overlap (due to the intra-group variability) was also estimated (right bottom pane) as described in Appendix A. Each quantitative assessment (bar graph) from the group of paw positioning features has been also transposed into a more visual representation (heat map) allowing for easier visual assessment of paw positioning distortion. Color scheme (blue to red) represents number of paw prints placed in the respective surface using the following scale from red corresponding to the highest and blue to zero count. Fig. 5B is the graphical representation of paw prints distribution with respect to the body center of animal in movement (heat map) for each genotype (WT, Pink1 KO and DJ-1 KO) at two different ages (4 and 8 months). On the two top panels, the four limbs have been represented with two normal oblong shapes for the hindlimbs and two smaller ones which even fused for the forelimbs at older age in WT animals. For Pink1 (middle panels) and DJ-1 KO (bottom panels), the hindlimb positioning surfaces have more the shapes of square and the zones between left and right are less defined as surfaces are merging. Same observation can be made for the forelimbs. This indicates less accuracy in limb positioning in space and a lack of coordination of the four limbs while animal is in movement. Quantitative measure of phenotype differences using pattern recognition approach were also obtained as described in Appendix A.

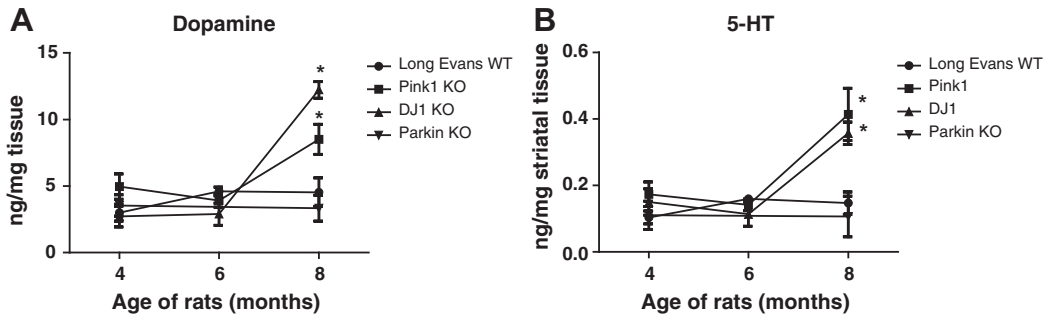

Fig. 6. Pink1 and DJ-1 KO rats have increased DA and 5-HT striatal content – left and right striata from homozygous Pink1 KO rats, homozygous DJ-1 KO rats, and WT rats (n = 6/group/age) were analyzed via ultra-high performance liquid chromatography-MS/MS for neurotransmitter content of dopamine, serotonin and their metabolites. Results showed a significant two- to three-fold increase in DA (6A) and 5-HT (6B) at 8 months of age in both Pink1 and DJ-1 KO rats. Parkin KO rats were not significantly different compared to WT. Data are represented as means ± SEM.*P < 0.01, significantly different from wild type, 2-way ANOVA, followed by Bonferroni multiple comparisons.

Pink1 and DJ-1 KO rats showed an abnormal paw positioning from the centre of the animals' body while in motion compared to WT rats translating by a lack of accuracy in positioning their limbs relative to the body's centre. Regarding gait dynamics, both lines at 4 and 8 month of age showed shorter duration in stride, swing and stance when compared to the age matched WT controlled animals (Discrimination and p values for Pink1 and DJ-1 respectively at 4 months: 83% ($p = 0.013$) and 84% ($p = 0.026$) and at 8 month: 89% ($p = 0.017$) and 90% ($p = 0.014$)) (Fig. 9) (see analysis for significant differences in Appendix A).

Neurochemical phenotyping of KO rats

At the end of the behavioral testing in the WIL Research study, left and right striata (n = 6/group/age) were collected, and ultra-high performance spectroscopy (UPLC)-MS/MS was used to measure concentrations of dopamine, serotonin, 3,4-dihydroxyphenylacetic acid (DOPAC), Homovanillic acid (HVA), and 5-Hydroxyindoleacetic acid (5-HIAA). Concentrations from left and right striata were averaged for each animal. There was a significant 2–3 fold increase in striatal dopamine in both KO rats at 8 months of age with significant effect of age $F(2, 45) = 35.28$, $p < 0.0001$, significant effect of genotype $F(2, 45) = 5.23$, $p = 0.0091$, and a significant interaction $F(4, 45) = 10.70$, $p < 0.0001$ (Fig. 6A).Similar to DA levels, striatal 5-HT levels also increased 2–3 fold at 8 months of age with significant effect of age $F(2, 45) = 18.39$, $p < 0.0001$, genotype $F(2, 45) = 5.90$, $p = 0.0053$, and a significant interaction between age and genotype $F(4, 45) = 4.29$, $p = 0.0051$ (Fig. 6B). Dopamine turnover was calculated by using the equation (DOPAC ± HVA/DA)*100. Serotonin turnover was calculated by using the equation (5-HIAA/5-HT)*100. There were no significant differences in the overall rate of DA or 5-HT turnover for either Pink1 or DJ-1 KO rats (data not shown). Parkin KO Rats were not significantly different from WT rats at any of the ages tested.

Pathological phenotyping of KO rats

At the end of the behavioral testing in the Wil Research study, brains were collected (n = 9/group/age), and immunohistochemistry was performed to examine tyrosine hydroxylase (TH) and alpha-synuclein (aSyn) staining. Nigral TH-immunoreactivity was substantially reduced in both Pink1 and DJ-1 KO rats at 6 months and 8 months of age compared to the WT rats (Fig. 7A). The ventral tegmental area (VTA) TH immunoreactivity remained unchanged at all ages. Unbiased stereology was performed to count the number of TH-positive neurons using Nissl as a counterstain for cell bodies. There were significant age-related decreases in numbers of TH positive neurons in SN of both Pink1 and DJ-1 KO rats (Fig. 7B). There was an average of 25% reduction at 6 months and over 50% reduction at 8 months of age in both genotypes with significant main effect for age $F(2, 72) = 14.31$, $p < 0.001$, and for genotype $F(2, 72) = 6.81$, $p = 0.0020$, and significant interaction of age and genotype $F(4, 72) = 3.37$, $p = 0.0139$. Parkin KO rats were not significantly different from WT rats even though there was a small 20% reduction observed at 8 months of age. To verify that this substantial loss of SNpc neurons represents neuronal loss rather than a loss of dopaminergic phenotype or simply a loss of TH expression, parallel Nissl counts were performed in the same sections to obtain total number of neurons in the 8-month old rats. The average total number of neurons in Long Evans WT rats was 54544 ± 3660. One-way ANOVA showed that there was a significant reduction (approximately 40%) in the total number of neurons in DJ-1 KO and Pink1 KO, but not Parkin KO rats $F(3, 32) = 16$, $p < 0.001$. The average for the total number of neurons for DJ-1, Pink1 and Parkin KO rats were 32240 ± 2553, 33348 ± 2701, and 51148 ± 2655, respectively. There are several factors as to the high counts of nigral cells reported in this study which complicate the comparison versus other publications. Methodological differences in delineation of SNpc boundaries, data collection (2d versus 3d), magnification (100× versus 3600×) or type of stereology (method-based versus design-based) can lead to differences in numbers of cell counted, even within the same tissue. The current study used design-based 3d stereology with high magnification (3600×), which may have resulted in higher neuronal counts compared to more recent publications (Cannon et al., 2013; Healy-Stoffel et al., 2012; Healy-Stoffel et al., 2013; Tapias et al., 2013)

Despite the robust and progressive loss of DA neurons in the SN pars compacta in both genotypes, there were no changes in TH-immuno reactivity in striatum at any of the three ages as quantified by optical densitometry (representative 8 month picture shown in Fig. 8). Staining for αSyn using antibody against total αSyn revealed no increase in the striatum or any other brain region in Pink1, DJ-1 or Parkin KO rats compared to WT (representative 8 month striatal staining shown in Fig. 8).

Discussion

The results of these studies demonstrate that loss of either Pink1 gene or DJ-1 gene produces a robust behavioral dysfunction and a significant loss of SN DA neurons in rats. Motor impairments in movement, strength and coordination precede nigral neuronal loss. The neurodegeneration is rapid between 4 and 8 months of age with about 50% decrease seen at 8 months of age. In both models, the nigral neurodegeneration does not correlate with changes in striatal TH or alpha-synuclein immunoreactivity; however, there is a 2-3 fold increase in both DA and 5-HT striatal content at 8 months of age in both rats models. Parkin KO rats were not different from WT rats in any of the behavioral, neurochemical and pathological outcome measures.

Mutations in Pink1, DJ-1 and Parkin genes, although rare, have been causally linked to early-onset PD presumably due to a loss of function of these genes (Bonifati et al., 2003; Kitada et al., 1998; Valente et al., 2004). The protein encoded by the Pink1 gene is a serine-threonine kinase, which has been suggested to provide protection against oxidative

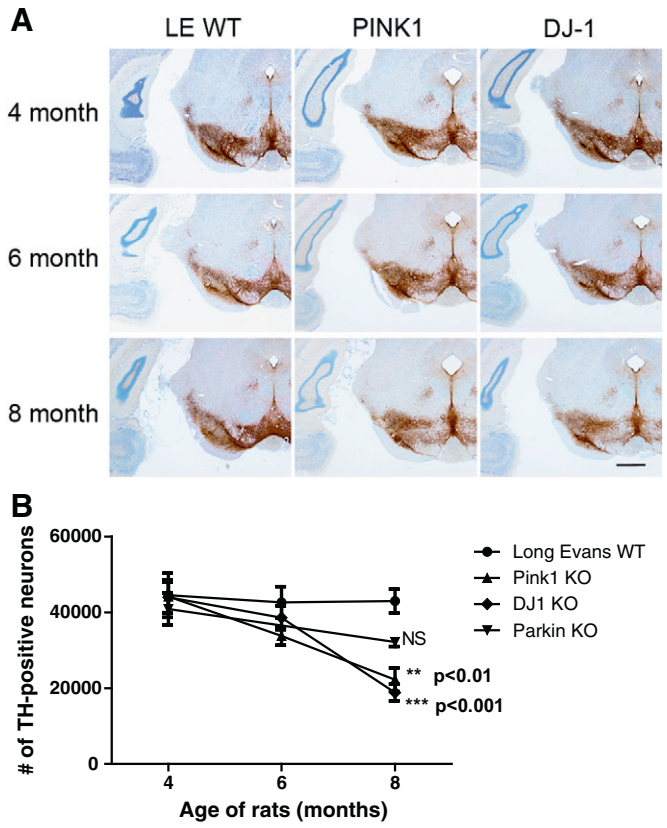

Fig. 7. Pink1 and DJ-1 KO rats exhibit a progressive loss of dopaminergic neurons in the Substantia nigra – homozygous pink1 KO rats, homozygous DJ-1 KO rats, and WT rats (n = 9/group/age) were perfused with paraformaldehyde. Fixed brains were sectioned and stained with tyrosine hydroxylase antibody and counterstained with Nissl stain to reveal cell bodies. Fig. 7A is representative staining from one rat from each of the three groups at each age. Immunohistological pictures show a progressive decrease in TH-immunoreactivity in the substantia nigra in both KO rats. Scale bar = 1 mm. Design-based unbiased stereology was used to identify and estimate neuronal number in the Substantia nigra pars compacta region using TH and Nissl staining. Fig. 7B shows that there was a significant and robust (greater than 50%) loss of nigral dopaminergic neurons between 4 and 8 months of age in both Pink1 and DJ-1 KO rats. Parkin KO rats were not significantly different from WT. Data are represented as means ± SEM.*P < 0.01, significantly different from wild type, 2-way ANOVA, followed by Bonferroni multiple comparisons.

stress by assisting in condemning damaged mitochondria to degradation/mitophagy and maintaining mitochondrial homeostasis (Springer and Kahle, 2011). Pink1 deficiency in mammalian neurons alters mitochondrial buffering capacity, increased reactive oxygen species and impaired respiration (Gandhi et al., 2009), suggesting a mechanism by which Pink1dysfunction would confer vulnerability to cell death. While the exact function(s) of DJ-1 protein have not been fully elucidated, it is thought to serve as a sensor of oxidative stress switching its isoelectric point to a more acidic form following oxidative stress (Mitsumoto and Nakagawa, 2001). Indeed, DJ-1 deficiency in various cell types including cultured mouse neurons, cell lines and DJ-1 patient derived lymphocytes led to mitochondrial dysfunction and increased sensitivity to oxidative stress (Irrcher et al., 2010). Parkin is an E3 ubiquitin ligase which has been shown to ubiquitinate substrates and to trigger proteasome-dependent degradation (Zhang et al., 2000), thus playing an important role in neuronal homeostatic processes. Accumulation of data over the years have suggested that these three protein enzymes serve to regulate mitochondrial function especially in response to oxidative stressors and that dysregulation of this function may confer vulnerability to nigral cell death (Cookson, 2010; Trempe and Fon, 2013). Due to the apparent loss of function mutations in these genes that may cause PD, genetic models based on gene knockout approaches may provide good construct validity.

Mouse knockout models of either Pink1 or DJ-1 gene have been shown to exhibit behavioral and neurochemical deficits, without a significant loss in nigral neurons and without any increase in total or aggregated alpha-synuclein. For example, mice lacking Pink1exhibited no change in dopaminergic neuron numbers, had normal dopamine concentration in the striatum and no changes in DA receptor density, however, evoked DA release from catecholamine terminals was greatly impaired (Kitada et al., 2007). DJ-1KO mice were reported to have behavioral dysfunction in motor activity, grip strength and progressive gait abnormalities despite lack of any pathological changes (Chandran et al., 2008). Parkin deficient mice displayed abnormal behavior in beam walk and adhesive removal tests, and a decrease in synaptic excitability in the striatum despite showing normal numbers of nigral dopaminergic neurons (Goldberg et al., 2003). Even mice lacking all three recessive genes of Pink1, DJ-1 and Parkin genes exhibited normal morphology and numbers of dopaminergic neurons up to 24 months of age (Kitada et al., 2009), suggesting that these three genes are not critical for survival of nigral neurons in the mouse.

In the current study, we observed normal numbers of dopamine neurons in the SN of both Pink1 and DJ-1 rats at 4 months of age as compared to Long Evans wild type, suggesting that the deficits observed at later ages were not developmental in origin. By 6 months of age, both Pink1 and DJ-1 KO rats started to show significant impairments in motor behaviors and these deficits persisted to 8 months of age. At the same time (6 months), nigral neuronal counts were only reduced by 25 percent indicating that behavioral deficits precede dopaminergic cell loss and that the behavior deficits may reflect neuronal dysfunction that likely occurs prior to loss of cell bodies in the SN. One possible explanation for such species differences could be the distribution and expression of these proteins in the rodent brain. However, neuroanatomical distribution of these proteins is similarly widespread and heterogeneous in both species (Bandopadhyay et al., 2005; Stichel et al., 2000; Taymans et al., 2006). It is also possible that the deficiency of one of these proteins leading to disruption of mitochondrial homeostasis confers higher vulnerability to aging-related oxidative

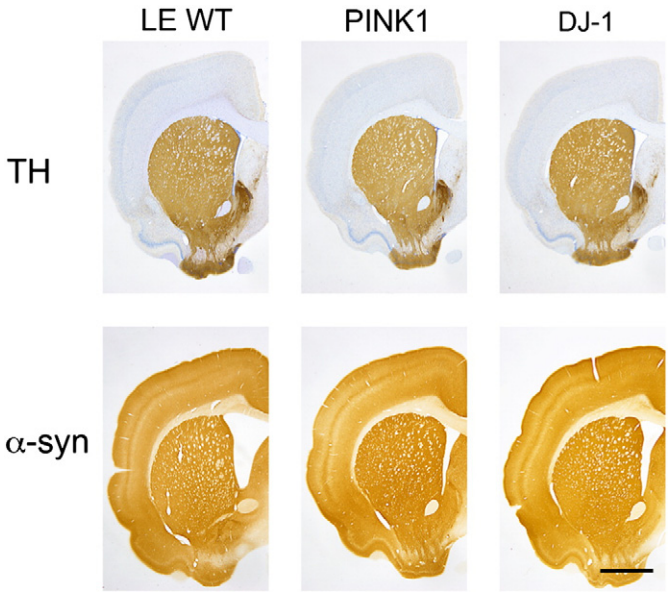

Fig 8. Pink1 and DJ-1 KO rats have no changes in TH or alpha-synuclein pathology in the striatum – homozygous pink1 KO rats, homozygous DJ-1 KO rats, and WT rats (n = 9/group/age) were perfused with paraformaldehyde. Fixed brains were sectioned and stained with antibodies against tyrosine hydroxylase or total alpha-synuclein. There were no changes observed in TH or alpha-synuclein immunoreactivity at any of the three ages. Representative pictures of rats from each of the three groups at 8 months of age are shown. Scale bar = 2 mm. There was no reduction in TH staining in the striatum despite robust loss of nigral neurons. There were no changes in alpha-synuclein immunoreactivity in the striatum.

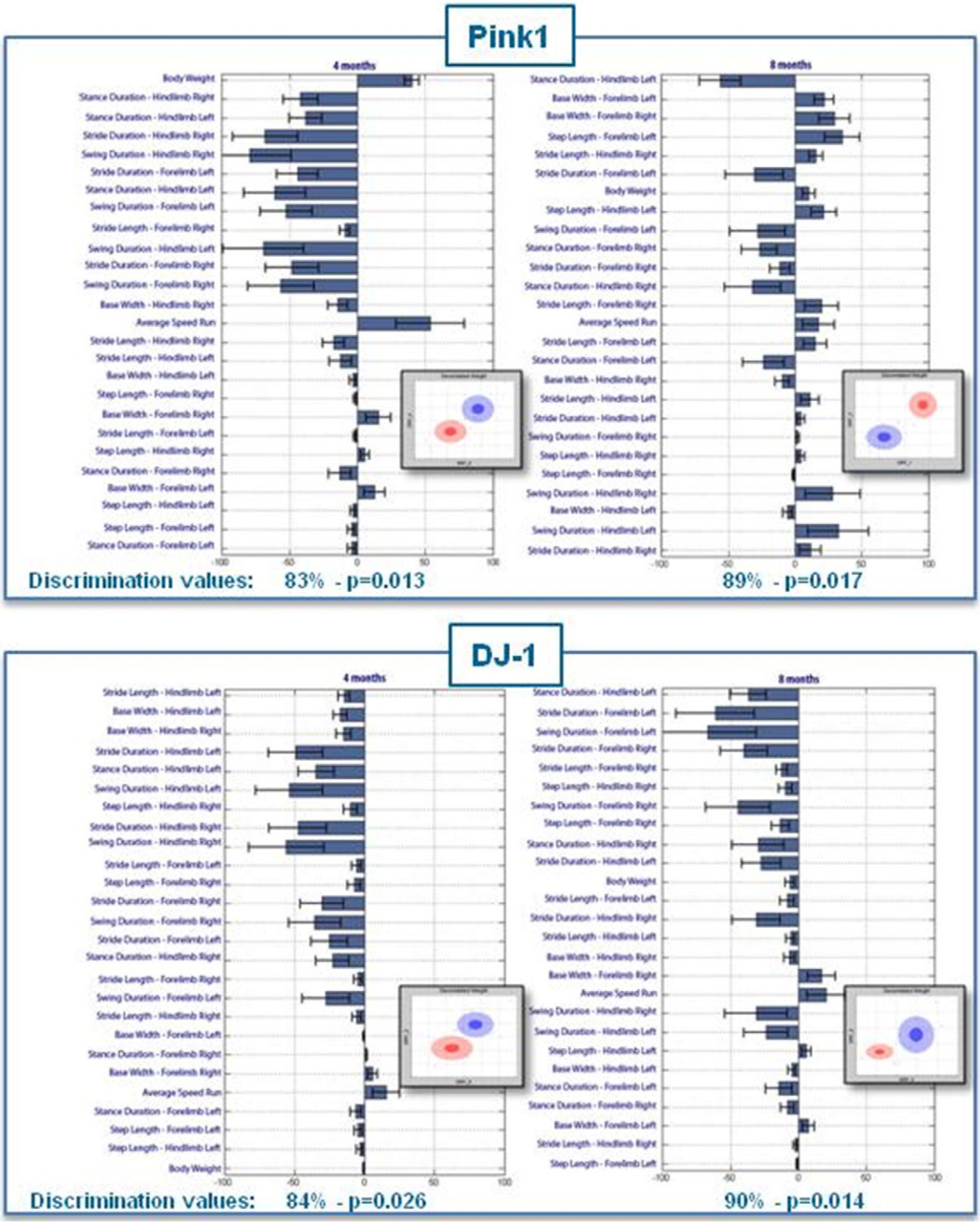

Fig. 9. Gait dynamic features analysis of Pink1 KO and DJ-1 KO at 4 and 8 months of age: The two top panels represent gait features difference of Pink1 KO compared to WT age matched control animals at 4 and 8 month of age. The two groups represented as a blue cloud (Pink1 KO) and a red cloud (WT) are well separated with a discrimination (and p) value of 83% ($p = 0.013$) and 89% ($p = 0.017$) at 4 and 8 months respectively. The two bottom panels represent gait features difference of DJ-1 KO compared to WT age matched control animals at 4 and 8 month of age. The two groups represented as a blue cloud (DJ-1 KO) and a red cloud (WT) are well separated with a discrimination (and p) value of 84% ($p = 0.026$) and 90% ($p = 0.014$) at 4 and 8 months respectively. Both lines show a faster gait dynamic (decrease in durations of stance, stride and swing) compared to WT control animals at 4 and 8 month of age.

stress in rats compared to mice. Few studies have explored such species differences in mitochondrial function (Lash et al., 2001; Panov et al., 2007); however, further systematic studies would need to explore differences due to species or strain as a function of gene deficiency in rats versus mice. Such studies could also shed light on the lack of any phenotype observed in Parkin KO rat despite robust phenotypic differences seen in Pink1 and DJ-1 KO rats compared to WT. It is possible given the trend in a small, albeit not significant, reduction in dopamine neurons, in 8 month old Parkin KO rats that a potential PD-like phenotype is delayed warranting further characterization in older aged rats.

Pink1 and DJ-1 KO rats do not display other features of clinical PD phenotype. In the current study, an increase in striatal dopamine was observed at the same time as gross behavioral dysfunction and fifty percent loss of nigral cells. Striatal dopamine levels have not always correlated with behavioral function in genetic models of PD. DJ-1 knockout mice that were reported to develop progressive behavioral abnormalities in gait, muscle strength and motor activity had normal

striatal dopamine function (Chandran et al., 2008), while others, in agreement with the current findings, have reported increased striatal dopamine content accompanying behavioral deficits (Chen et al., 2005; Manning-Bog et al., 2007). Increased dopamine function at the level of the striatum has been proposed as functional presynaptic compensation resulting from nigrostriatal damage (Eberling et al., 1997; Hornykiewicz, 2001). Indeed, many parameters of striatal dopamine function such as total content, release, turnover, and uptake have been shown to be significantly increased after nigral cell loss (Snyder et al., 1990; Zigmond et al., 1984). However, this compensation seems to be linked to the degree and severity of the nigrostriatal damage, with moderate lesions of the nigra producing an increase in dopamine, and progressively severe lesions resulting in eventual reduction in striatal dopamine, as seen with unilateral 6-OHDA lesion in the rat (Bergstrom et al., 2001) and MPTP lesion in the squirrel monkey (Perez et al., 2008). Based on these findings, it is possible that phenotypic characterization of Pink1 and DJ-1 KO rats at later ages may show more severe neurodegeneration and lower striatal dopamine function. The concurrent increase in striatal 5-HT content in the current study may be part of compensatory changes proposed to happen in non-basal ganglia related structures and non-catecholamine circuitries that feed into and out of the nigrostriatal system (Bezard et al., 2001). In support of this hypothesis, several studies of dopamine depletion have reported an increase in 5-HT neuronal firing (Wang et al., 2009), serotonergic innervation (Guerra et al., 1997), and similar to the current study, an increase in 5-HT concentration without a change in metabolite 5-HIAA levels (Hennis et al., 2014). Alternatively, Pink1 and DJ-1 genes may affect 5-HT function independently of the nigrostriatal neurodegeneration, by directly influencing vescicular and presynaptic function through mitochondria activity and energy maintenance (Morais et al., 2009; Usami et al., 2011). Future studies determining evoked release, synaptic connectivity, axonal swellings, or other measures of neurotransmitter system integrity(such as DAT, VMAT, NET, SERT binding) may shed more light on whether early striatal dysfunction is correlated with early behavioral deficits observed in these models.

In the preliminary analyses performed for synuclein staining, there was no change in alpha-synuclein immunoreactivity within the SN, striatum or any other brain areas in Pink1, or DJ-1KO rats suggesting that synuclein pathology may not be directly responsible for the neurodegeneration observed in these KO rats. Due to the lack of reports of post-mortem examinations of patients with DJ-1 mutations (Cookson, 2010), we do not yet know the severity of neuronal loss or whether they have Lewy bodies. Recent pathological studies have shown Lewy bodies in Pink1-linked Parkinsonism and some cases of Parkin-linked Parkisonism (Farrer et al., 2001; Miyakawa et al., 2013; Poulopoulos et al., 2012; Pramstaller et al., 2005; Samaranch et al., 2010; Sasaki et al., 2004). In the context of current findings, more stringent characterization of protein levels (e.g. proteinase-K digestion) with antibodies to different epitopes, antibodies against different species, and antibodies against pathological phosphorylated species need to be performed in future to confirm absence of synuclein pathology.

The current behavioral, neurochemical and pathological characterization was intended as a basic collection of essential PD-relevant phenotypic data. MJFF hopes that the availability of these animals will better position the research community to conduct more specialized, detailed and extensive characterization that caters to different research interests. In summary, our findings from single KO rat studies demonstrate that lack of either Pink1 or DJ-1 protein is sufficient to cause dopaminergic neurodegeneration in rats. These results support the conclusion that these proteins are critical for survival of nigral neurons in rats. Furthermore, absence of these proteins results in gross motor impairments in several behavioral outcome measures in rats. The results of this study support the use of the Pink1 and DJ-1 KO rat models for elucidating biological and pathological changes that occur in autosomal recessive, early onset PD and provide a critical research tool to explore therapeutic approaches.

Conflict of interest

None

Acknowledgements

The authors would like to acknowledge several individuals that were responsible for the coordination and management efforts around generation, transfer of rats and rat tissues, characterization as well as data collection/validation: Edward Weinstein, Diana Ji, and Lara Little at SAGE Labs (Saint Louis, MO), Lori Lankow at Sigma (Saint Louis, MO), Julie Varsho at WIL Research (Ashland, OH), Dr. Vadim Alexandrov (Psychogenics), Hunter Greis, Yasmin Aziz and Brennan Long at MJFF (New York, NY). Finally, we would like to thank all the Parkinson's disease patients and our donors that continue to inspire us with their endless optimism.

Appendix A. Quantitative assessment of disease phenotype using De-correlated ranked feature analysis (DRFA)

The outcome from PsychoGenics' automated platforms (NeuroCube as well as from other "Cubes") is a large set of features (behavioral parameters) that can be used for various analyses. Many of these features are correlated. Therefore, we form statistically independent combinations of the original features (further referred to as *de-correlated features*). Each de-correlated feature extracts information from the whole cluster of the original features, so the new feature space has lower dimensionality.

Next, we apply a proprietary feature ranking algorithm to score each feature discrimination power (ability to separate the two groups, e.g. control and disease). Ranking is an important part of our analyses because it weighs each feature change by its relevance for discrimination of these particular two groups: if there is a significant change in some irrelevant feature measured for a particular phenotype, the

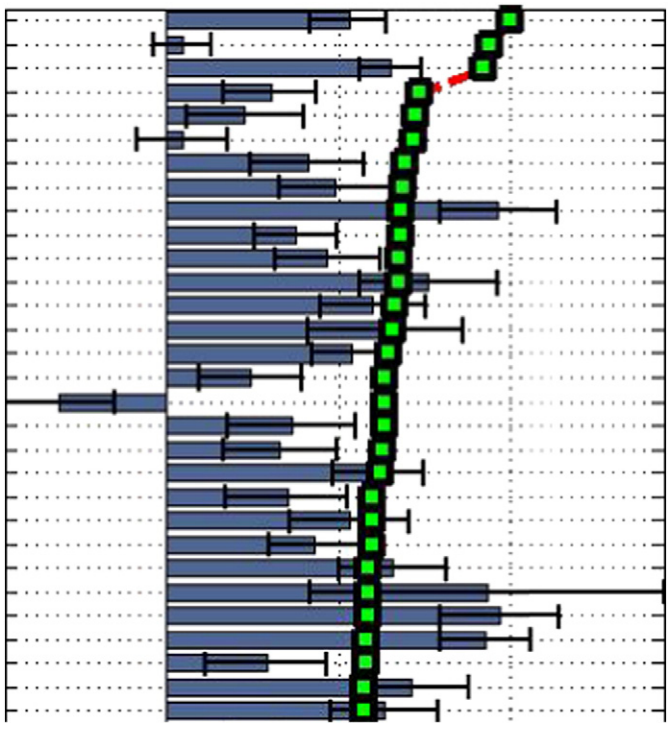

Fig. A1. Difference in feature values and feature ranks (red curve with green squares). Relative difference (%) between feature values in two different sets is calculated and plotted in the order corresponding to feature ranks together with their ranks varying from 0 to 100%.

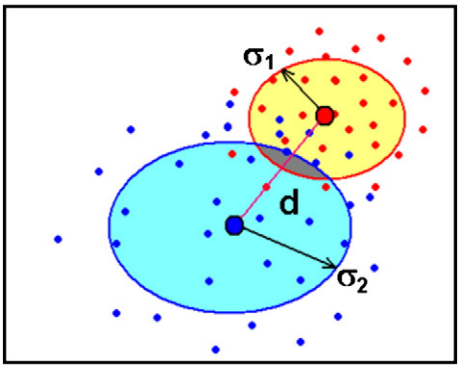

Fig. A2. Visualization of binary discrimination in the ranked de-correlated feature space. The two highest ranked de-correlated features are chosen to form the 2D coordinate plane for visualization purposes. Each dot represents a mouse. Mice from the control group are shown as blue dots and mice from the disease group are plotted in red. The other convenient (from the scale perspective) but totally equivalent measure derived from the cloud overlap is discrimination probability = 1 – overlap, which measures how reliably a classifier can be trained to discriminate between groups A and B above the chance level, zero corresponding to 100% overlap and no ability to distinguish the two groups above the chance level, whereas 100% meaning the error free discrimination.

low rank of this feature will automatically reduce the effect of such change in our analyses, so we don't have to resort to the conventional "feature selection" approach and discard information buried in the less informative features.

Ranking algorithm can be applied to either original or the new features to gain insight about the key control-disease differences (see Fig. A1).

Feature analysis: quantitative assessment of disease phenotype

In the new feature space, the overlap between the "clouds" (Gaussian distributions approximating the groups of mice in the ranked de-correlated features space) serves as a quantitative measure of *separability ("distinguishability")* between the two groups (see Fig. A2). For visualization purposes, we plot each cloud with its semi-axes equal to the one standard deviation along the corresponding dimensions. Note, however, that while the overlap between any two Gaussian distributions is always non-zero, it may not necessarily be seen at the "1-sigma level".

Statistical significance of the discrimination value can be estimated in the following way. First, each labeled set of subjects is randomly split with 1:3 ratio, where larger groups from each set are used to calculate discrimination probability calculated with the procedure described above. This procedure is repeated multiple times with different random splitting for each iteration to build distribution of "true" discrimination probability p_{true} as shown in green color in Fig. A3 (step 1). Next, all subjects from both groups are combined together without individual class labels (step 2). Similarly to the previous step, this set is split randomly multiple times. After many iterations, distribution of "random" discrimination probability p_{random} is built as shown in cyan color in Fig. A3 (step 2). Both distributions are normalized and their mutual weighted overlap is calculated. The resulting value is a generalized quantity of what is well known as p-value of statistical significance.

References

Bandopadhyay, R., Miller, D.W., Kingsbury, A.E., Jowett, T.P., Kaleem, M.M., Pittman, A.M., de, S.R., Cookson, M.R., Lees, A.J., 2005. Development, characterisation and epitope mapping of novel monoclonal antibodies for DJ-1 (PARK7) protein. Neurosci. Lett. 383, 225–230.

Baptista, M.A., Dave, K.D., Sheth, N.P., De Silva, S.N., Carlson, K.M., Aziz, Y.N., Fiske, B.K., Sherer, T.B., Frasier, M.A., 2013. A strategy for the generation, characterization and distribution of animal models by The Michael J. Fox Foundation for Parkinson's Research. Dis. Model Mech. 6, 1316–1324.

Bergstrom, B.P., Schertz, K.E., Weirick, T., Nafziger, B., Takacs, S.A., Lopes, K.O., Massa, K.J., Walker, Q.D., Garris, P.A., 2001. Partial, graded losses of dopamine terminals in the rat caudate-putamen: an animal model for the study of compensatory adaptation in preclinical parkinsonism. J. Neurosci. Methods 106, 15–28.

Bezard, E., Crossman, A.R., Gross, C.E., Brotchie, J.M., 2001. Structures outside the basal ganglia may compensate for dopamine loss in the presymptomatic stages of Parkinson's disease. FASEB J. 15, 1092–1094.

Bonifati, V., Rizzu, P., van Baren, M.J., Schaap, O., Breedveld, G.J., Krieger, E., Dekker, M.C., Squitieri, F., Ibanez, P., Joosse, M., van Dongen, J.W., Vanacore, N., van Swieten, J.C., Brice, A., Meco, G., van Duijn, C.M., Oostra, B.A., Heutink, P., 2003. Mutations in the DJ-1 gene associated with autosomal recessive early-onset parkinsonism. Science 299, 256–259.

Cannon, J.R., Geghman, K.D., Tapias, V., Sew, T., Dail, M.K., Li, C., Greenamyre, J.T., 2013. Expression of human E46K-mutated alpha-synuclein in BAC-transgenic rats replicates early-stage Parkinson's disease features and enhances vulnerability to mitochondrial impairment. Exp. Neurol. 240, 44–56.

Carbery, I.D., Ji, D., Harrington, A., Brown, V., Weinstein, E.J., Liaw, L., Cui, X., 2010. Targeted genome modification in mice using zinc-finger nucleases. Genetics 186, 451–459.

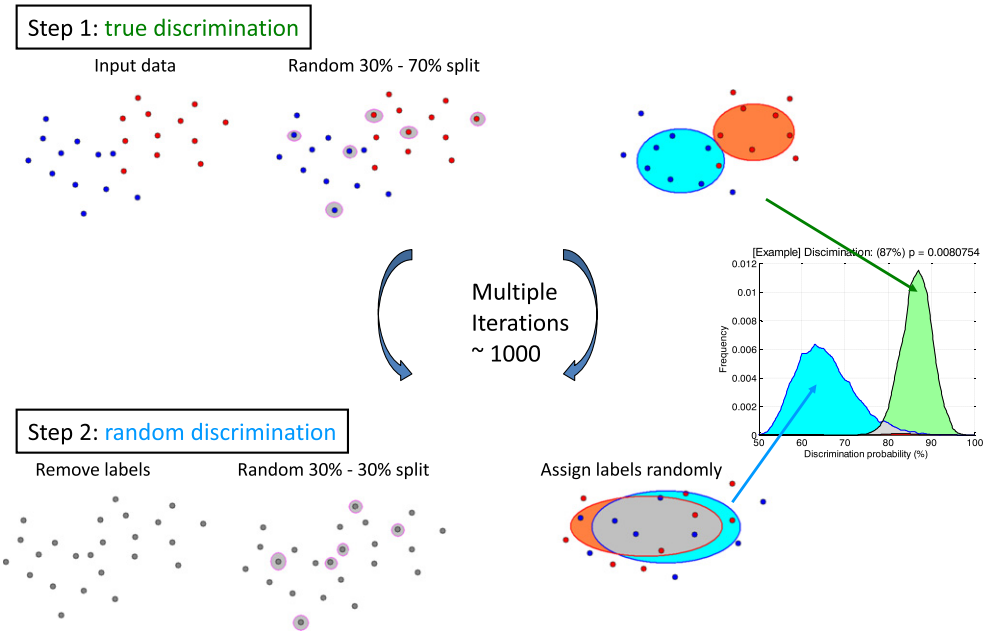

Fig. A3. Calculation of discrimination significance.

Chandran, J.S., Lin, X., Zapata, A., Hoke, A., Shimoji, M., Moore, S.O., Galloway, M.P., Laird, F. M., Wong, P.C., Price, D.L., Bailey, K.R., Crawley, J.N., Shippenberg, T., Cai, H., 2008. Progressive behavioral deficits in DJ-1-deficient mice are associated with normal nigrostriatal function. Neurobiol. Dis. 29, 505–514.
Chen, L., Cagniard, B., Mathews, T., Jones, S., Koh, H.C., Ding, Y., Carvey, P.M., Ling, Z., Kang, U.J., Zhuang, X., 2005. Age-dependent motor deficits and dopaminergic dysfunction in DJ-1 null mice. J. Biol. Chem. 280, 21418–21426.
Cookson, M.R., 2010. DJ-1, PINK1, and their effects on mitochondrial pathways. Mov. Disord. 25 (Suppl. 1), S44–S48.
Eberling, J.L., Bankiewicz, K.S., Jordan, S., VanBrocklin, H.F., Jagust, W.J., 1997. PET studies of functional compensation in a primate model of Parkinson's disease. Neuroreport 8, 2727–2733.
Farrer, M.J., 2006. Genetics of Parkinson disease: paradigm shifts and future prospects. Nat. Rev. Genet. 7, 306–318.
Farrer, M., Chan, P., Chen, R., Tan, L., Lincoln, S., Hernandez, D., Forno, L., Gwinn-Hardy, K., Petrucelli, L., Hussey, J., Singleton, A., Tanner, C., Hardy, J., Langston, J.W., 2001. Lewy bodies and parkinsonism in families with parkin mutations. Ann. Neurol. 50, 293–300.
Gaj, T., Guo, J., Kato, Y., Sirk, S.J., Barbas III, C.F., 2012. Targeted gene knockout by direct delivery of zinc-finger nuclease proteins. Nat. Methods 9, 805–807.
Gandhi, S., Wood-Kaczmar, A., Yao, Z., Plun-Favreau, H., Deas, E., Klupsch, K., Downward, J., Latchman, D.S., Tabrizi, S.J., Wood, N.W., Duchen, M.R., Abramov, A.Y., 2009. PINK1-associated Parkinson's disease is caused by neuronal vulnerability to calcium-induced cell death. Mol. Cell 33, 627–638.
Geurts, A.M., et al., 2009. Knockout rats via embryo microinjection of zinc-finger nucleases. Science 325, 433.
Goldberg, M.S., Fleming, S.M., Palacino, J.J., Cepeda, C., Lam, H.A., Bhatnagar, A., Meloni, E. G., Wu, N., Ackerson, L.C., Klapstein, G.J., Gajendiran, M., Roth, B.L., Chesselet, M.F., Maidment, N.T., Levine, M.S., Shen, J., 2003. Parkin-deficient mice exhibit nigrostriatal deficits but not loss of dopaminergic neurons. J. Biol. Chem. 278, 43628–43635.
Goldberg, M.S., Pisani, A., Haburcak, M., Vortherms, T.A., Kitada, T., Costa, C., Tong, Y., Martella, G., Tscherter, A., Martins, A., Bernardi, G., Roth, B.L., Pothos, E.N., Calabresi, P., Shen, J., 2005. Nigrostriatal dopaminergic deficits and hypokinesia caused by inactivation of the familial Parkinsonism-linked gene DJ-1. Neuron 45, 489–496.
Guerra, M.J., Liste, I., Labandeira-Garcia, J.L., 1997. Effects of lesions of the nigrostriatal pathway and of nigral grafts on striatal serotonergic innervation in adult rats. Neuroreport 8, 3485–3488.
Healy-Stoffel, M., Ahmad, S.O., Stanford, J.A., Levant, B., 2012. A novel use of combined tyrosine hydroxylase and silver nucleolar staining to determine the effects of a unilateral intrastriatal 6-hydroxydopamine lesion in the substantia nigra: a stereological study. J. Neurosci. Methods 210, 187–194.
Healy-Stoffel, M., Ahmad, S.O., Stanford, J.A., Levant, B., 2013. Altered nucleolar morphology in substantia nigra dopamine neurons following 6-hydroxydopamine lesion in rats. Neurosci. Lett. 546, 26–30.
Hennis, M.R., Marvin, M.A., Taylor, C.M., Goldberg, M.S., 2014. Surprising behavioral and neurochemical enhancements in mice with combined mutations linked to Parkinson's disease. Neurobiol. Dis. 62, 113–123.
Hornykiewicz, O., 2001. Chemical neuroanatomy of the basal ganglia – normal and in Parkinson's disease. J. Chem. Neuroanat. 22, 3–12.
Houlden, H., Singleton, A.B., 2012. The genetics and neuropathology of Parkinson's disease. Acta Neuropathol. 124, 325–338.
Irrcher, I., et al., 2010. Loss of the Parkinson's disease-linked gene DJ-1 perturbs mitochondrial dynamics. Hum. Mol. Genet. 19, 3734–3746.
Kitada, T., Asakawa, S., Hattori, N., Matsumine, H., Yamamura, Y., Minoshima, S., Yokochi, M., Mizuno, Y., Shimizu, N., 1998. Mutations in the parkin gene cause autosomal recessive juvenile parkinsonism. Nature 392, 605–608.
Kitada, T., Pisani, A., Porter, D.R., Yamaguchi, H., Tscherter, A., Martella, G., Bonsi, P., Zhang, C., Pothos, E.N., Shen, J., 2007. Impaired dopamine release and synaptic plasticity in the striatum of PINK1-deficient mice. Proc. Natl. Acad. Sci. U. S. A. 104, 11441–11446.
Kitada, T., Tong, Y., Gautier, C.A., Shen, J., 2009. Absence of nigral degeneration in aged parkin/DJ-1/PINK1 triple knockout mice. J. Neurochem. 111, 696–702.
Lash, L.H., Qian, W., Putt, D.A., Hueni, S.E., Elfarra, A.A., Krause, R.J., Parker, J.C., 2001. Renal and hepatic toxicity of trichloroethylene and its glutathione-derived metabolites in rats and mice: sex-, species-, and tissue-dependent differences. J. Pharmacol. Exp. Ther. 297, 155–164.
Lees, A.J., Hardy, J., Revesz, T., 2009. Parkinson's disease. Lancet 373, 2055–2066.
Manning-Bog, A.B., Caudle, W.M., Perez, X.A., Reaney, S.H., Paletzki, R., Isla, M.Z., Chou, V.P., McCormack, A.L., Miller, G.W., Langston, J.W., Gerfen, C.R., Dimonte, D.A., 2007. Increased vulnerability of nigrostriatal terminals in DJ-1-deficient mice is mediated by the dopamine transporter. Neurobiol. Dis. 27, 141–150.
Martin, I., Dawson, V.L., Dawson, T.M., 2011. Recent advances in the genetics of Parkinson's disease. Annu. Rev. Genomics Hum. Genet. 12, 301–325.
Mitsumoto, A., Nakagawa, Y., 2001. DJ-1 is an indicator for endogenous reactive oxygen species elicited by endotoxin. Free Radic. Res. 35, 885–893.
Miyakawa, S., Ogino, M., Funabe, S., Uchino, A., Shimo, Y., Hattori, N., Ichinoe, M., Mikami, T., Saegusa, M., Nishiyama, K., Mori, H., Mizuno, Y., Murayama, S., Mochizuki, H., 2013. Lewy body pathology in a patient with a homozygous parkin deletion. Mov. Disord. 28, 388–391.
Morais, V.A., Verstreken, P., Roethig, A., Smet, J., Snellinx, A., Vanbrabant, M., Haddad, D., Frezza, C., Mandemakers, W., Vogt-Weisenhorn, D., Van, C.R., Wurst, W., Scorrano, L., De, S.B., 2009. Parkinson's disease mutations in PINK1 result in decreased Complex I activity and deficient synaptic function. EMBO Mol. Med. 1, 99–111.
Panov, A., Dikalov, S., Shalbuyeva, N., Hemendinger, R., Greenamyre, J.T., Rosenfeld, J., 2007. Species- and tissue-specific relationships between mitochondrial permeability transition and generation of ROS in brain and liver mitochondria of rats and mice. Am. J. Physiol. Cell Physiol. 292, C708–C718.
Perez, X.A., Parameswaran, N., Huang, L.Z., O'Leary, K.T., Quik, M., 2008. Pre-synaptic dopaminergic compensation after moderate nigrostriatal damage in non-human primates. J. Neurochem. 105, 1861–1872.
Poulopoulos, M., Levy, O.A., Alcalay, R.N., 2012. The neuropathology of genetic Parkinson's disease. Mov. Disord. 27, 831–842.
Pramstaller, P.P., Schlossmacher, M.G., Jacques, T.S., Scaravilli, F., Eskelson, C., Pepivani, I., Hedrich, K., Adel, S., Gonzales-McNeal, M., Hilker, R., Kramer, P.L., Klein, C., 2005. Lewy body Parkinson's disease in a large pedigree with 77 Parkin mutation carriers. Ann. Neurol. 58, 411–422.
Prusky, G.T., Harker, K.T., Douglas, R.M., Whishaw, I.Q., 2002. Variation in visual acuity within pigmented, and between pigmented and albino rat strains. Behav. Brain Res. 136, 339–348.
Rousseaux, M.W., Marcogliese, P.C., Qu, D., Hewitt, S.J., Seang, S., Kim, R.H., Slack, R.S., Schlossmacher, M.G., Lagace, D.C., Mak, T.W., Park, D.S., 2012. Progressive dopaminergic cell loss with unilateral-to-bilateral progression in a genetic model of Parkinson disease. Proc. Natl. Acad. Sci. U. S. A. 109, 15918–15923.
Samaranch, L., Lorenzo-Betancor, O., Arbelo, J.M., Ferrer, I., Lorenzo, E., Irigoyen, J., Pastor, M.A., Marrero, C., Isla, C., Herrera-Henriquez, J., Pastor, P., 2010. PINK1-linked parkinsonism is associated with Lewy body pathology. Brain 133, 1128–1142.
Sasaki, S., Shirata, A., Yamane, K., Iwata, M., 2004. Parkin-positive autosomal recessive juvenile Parkinsonism with alpha-synuclein-positive inclusions. Neurology 63, 678–682.
Snyder, G.L., Keller Jr., R.W., Zigmond, M.J., 1990. Dopamine efflux from striatal slices after intracerebral 6-hydroxydopamine: evidence for compensatory hyperactivity of residual terminals. J. Pharmacol. Exp. Ther. 253, 867–876.
Springer, W., Kahle, P.J., 2011. Regulation of PINK1-Parkin-mediated mitophagy. Autophagy 7, 266–278.
Sterio, D.C., 1984. The unbiased estimation of number and sizes of arbitrary particles using the disector. J. Microsc. 134, 127–136.
Stichel, C.C., Augustin, M., Kuhn, K., Zhu, X.R., Engels, P., Ullmer, C., Lubbert, H., 2000. Parkin expression in the adult mouse brain. Eur. J. Neurosci. 12, 4181–4194.
Sun, J., Kouranova, E., Cui, X., Mach, R.H., Xu, J., 2013. Regulation of dopamine presynaptic markers and receptors in the striatum of DJ-1 and Pink1 knockout rats. Neurosci. Lett. 557 Pt B, 123–128.
Tapias, V., Greenamyre, J.T., Watkins, S.C., 2013. Automated imaging system for fast quantitation of neurons, cell morphology and neurite morphometry in vivo and in vitro. Neurobiol. Dis. 54, 158–168.
Taymans, J.M., Van den Haute, C., Baekelandt, V., 2006. Distribution of PINK1 and LRRK2 in rat and mouse brain. J. Neurochem. 98, 951–961.
Trempe, J.F., Fon, E.A., 2013. Structure and Function of parkin, PINK1, and DJ-1, the three musketeers of neuroprotection. Front. Neurol. 4, 38.
Usami, Y., Hatano, T., Imai, S., Kubo, S., Sato, S., Saiki, S., Fujioka, Y., Ohba, Y., Sato, F., Funayama, M., Eguchi, H., Shiba, K., Ariga, H., Shen, J., Hattori, N., 2011. DJ-1 associates with synaptic membranes. Neurobiol. Dis. 43, 651–662.
Valente, E.M., Salvi, S., Ialongo, T., Marongiu, R., Elia, A.E., Caputo, V., Romito, L., Albanese, A., Dallapiccola, B., Bentivoglio, A.R., 2004. PINK1 mutations are associated with sporadic early-onset parkinsonism. Ann. Neurol. 56, 336–341.
Wang, S., Zhang, Q.J., Liu, J., Wu, Z.H., Wang, T., Gui, Z.H., Chen, L., Wang, Y., 2009. Unilateral lesion of the nigrostriatal pathway induces an increase of neuronal firing of the midbrain raphe nuclei 5-HT neurons and a decrease of their response to 5-HT(1A) receptor stimulation in the rat. Neuroscience 159, 850–861.
West, M.J., Slomianka, L., Gundersen, H.J., 1991. Unbiased stereological estimation of the total number of neurons in thesubdivisions of the rat hippocampus using the optical fractionator. Anat. Rec. 231, 482–497.
Zhang, Y., Gao, J., Chung, K.K., Huang, H., Dawson, V.L., Dawson, T.M., 2000. Parkin functions as an E2-dependent ubiquitin- protein ligase and promotes the degradation of the synaptic vesicle-associated protein, CDCrel-1. Proc. Natl. Acad. Sci. U. S. A. 97, 13354–13359.
Zigmond, M.J., Acheson, A.L., Stachowiak, M.K., Stricker, E.M., 1984. Neurochemical compensation after nigrostriatal bundle injury in an animal model of preclinical parkinsonism. Arch. Neurol. 41, 856–861.